General Disclaimer

One or more of the Following Statements may affect this Document

- This document has been reproduced from the best copy furnished by the organizational source. It is being released in the interest of making available as much information as possible.

- This document may contain data, which exceeds the sheet parameters. It was furnished in this condition by the organizational source and is the best copy available.

- This document may contain tone-on-tone or color graphs, charts and/or pictures, which have been reproduced in black and white.

- This document is paginated as submitted by the original source.

- Portions of this document are not fully legible due to the historical nature of some of the material. However, it is the best reproduction available from the original submission.

UAH Research Report No. 175

MULTIFLUIDS DESCRIPTION OF DYNAMICS OF UPPER ATMOSPHERE

by

S. T. Wu and R. J. Hung

Final Technical Report

This research work was supported by
the National Aeronautics and Space Administration
George C. Marshall Space Flight Center
Contract NAS8-29543

Submitted by

The University of Alabama in Huntsville
School of Graduate Studies and Research
P. O. Box 1247
Huntsville, Alabama 35807

July 1975

ACKNOWLEDGEMENT

This work was supported by the NASA/Marshall Space Flight Center under Contract NAS8-29543, with the technical coordination of Drs. R. E. Smith and Gary R. Swenson, Space Environment Branch/Space Sciences Laboratory. Their encouragement and consultation during the course of this study are highly appreciated.

The manuscript was typed by Mrs. Carol Holladay. Her skillful typing and patience are greatly appreciated.

TABLE OF CONTENTS

CHAPTER I

SUMMARY

A multifluids model to investigate ionospheric dynamics has been established on kinetic theory. Its resultant equations are used to examine the following dynamic problems in the γ region of 80 - 2000 Km of the ionosphere:

i) Propagation of acoustic modes in the 500-2,000 Km of the ionosphere (two fluid model).

ii) The relation between the cross field plasma drift instabilities and type I and type II ionospheric irregularities.

iii) Time dependent neutral wind structure and horizontal pressure gradient.

In these studies, we have found out that case (i), the dissipation of acoustic waves by electrons, is through the viscous and thermal conduction effects and ion is through Landau damping in the region of 500-2,000 Km of the ionosphere; the type I ionospheric irregularity (case (ii)) can be excited by either temperature gradient or density gradient along the vertical height, and the type II ionospheric irregularity can only be generated by temperature gradients; case (iii), the ion drift, will initiate neutral motion in an early stage of development; however, the neutrals will also drive the ions in a later stage.

CHAPTER II
TWO-FLUIDS DESCRIPTION OF PROPAGATION OF ACOUSTIC MODES IN THE REGION OF 500-2000 KM IONOSPHERE*

II-1 General Statement of the Problem

Propagation of acoustic waves in the upper atmosphere of the earth reflects the thermal fluctuations of the motions of the upper atmosphere. The investigation of the characteristics of the propagation and dissipation of acoustic-mode waves is of particular interest to environmental perturbation and to plasma physics laboratory definition and also in the design and operation of the space shuttle.

The physical properties of the medium in which waves propagate affect the characteristics of the wave propagation. In particular, wave propagation is governed by the transport phenomena of the medium which depend on collision effects of particles and waves. As the acoustic modes propagate in the various altitudes of the atmosphere, the characteristics of the wave propagation vary from region to region because the physical parameters of the medium also change. In the lower altitude region, the atmosphere contains more neutral molecules than ionized particles. As altitude increases, the particle ionization increases. In the meanwhile, neutral-neutral, ion-neutral and electron-neutral collision frequencies decrease. As the altitude reaches 500 Km, the electron collision frequency is $400\,sec^{-1}$, the ion collision frequency is $0.1\,sec^{-1}$, and the neutral collision frequency is $4 \times 10^{-2}\ sec^{-1}$ (Hanson 1965; U.S. Standard Atmosphere, 1962). In other words, the effect of neutral particles on the propagation of acoustic waves with wave periods 0.01 to 10 seconds (or wave frequencies 0.1 to 100 Hz) is negligible in the altitude above 500 Km. Thus, at altitudes above 500 Km, the collision effect due to neutral particles disappears, and we have to consider Coulomb collisions instead of neutral particle collisions.

As we have mentioned earlier, propagation of waves is modified by transport effects due to either particle collisions or Coulomb collisions. In the lower altitude atmosphere where the neutral particles dominate, the transport coefficients of

*A portion of the results are published in the J. of Geophysical Research (1975).

viscosity and thermal conduction from kinetic theory (Chapman and Cowling, 1960) are

$$\mu = 1.27 \frac{nT}{\nu_{n-n}}$$

$$K = \frac{1}{4} C_v \mu (9\gamma - 5)$$

where μ, K, n, and T denote viscosity, thermal conductivity, number density and temperature, respectively, and C_v, γ and ν_{n-n} denote specific heat at constant volume, the ratio of specific heats, and the neutral-neutral collision frequency, respectively. In the collision-dominated regions, such as the D, E, and lower F regions of the ionosphere, order of magnitude estimations show that both thermal conduction and viscosity have a negligible effect on the propagation of waves with periods from 0.01 to 10 seconds. As the altitude increases, the collision frequency becomes smaller and both thermal conduction and viscosity become significant. Thus, at the higher altitudes the acoustic modes suffer from strong dissipation effects due to thermal conduction and viscosity. This implies that the acoustic modes might not propagate very long distances without being damped out. It seems that this conclusion was reached too fast. In order to have a better understanding of the physics of acoustic mode propagation in the upper atmosphere, particularly in the transitional region from the collisional to the collisionless situation, a new approach based on kinetic theory should be considered.

As our primary interest is in investigating the acoustic modes propagation in the upper atmosphere where particle transition from collisional to collisionless conditions occurs, our problem is to investigate modes with wave periods from 0.01 to 10 seconds propagating in the altitude region from 500 Km to 2000 Km. In this region, isotropic electrons are in transitional between the collisional to collisionless states, while the anistropic ions are in a collisionless state. Our primary consideration shall be limited to wave propagation in the medium of the ionized plasma rather than the neutral particles because the effect of neutral particle collisions is negligible in this region. The propagation of acoustic modes in the ionized particles has been studied for several years. For the case of wave propagation in a collision-dominated fully ionized plasma, a comprehensive study

was done by Braginskii (1965). For the acoustic mode propagation in a collisionless fully ionized plasma, interesting results were obtained by Bernstein and Trehan (1960). In a study of acoustic wave propagation in the medium of ionized particles without a magnetic field, Bhatnager, Gross and Krook (1954) presented a model of single species rarefied ionized particles, and Gross and Krook (1956) showed a model of two-component ionized gas. In the study of the dynamics of rarefied neutral particles, Hamel (1965) accomplished an investigation of a binary gas mixture and Holway (1966) proposed a statistical model with a multicomponent gas mixture. To investigate the acoustic wave propagation in the transitional ionosphere, Tolstoy (1972) suggested that continuum theory is inadequate and a more sophisticated treatment based on an adequate molecular model combined with Boltzmann's equation should be adopted.

In the present study, we propose to investigate acoustic mode propagation in the upper atmosphere from 500 to 2000 Km altitude, where electrons behave as if they are in a transition state between a collisional and a collisionless state, while the ions act as though they are in a collisionless regime for waves with periods of 0.01 to 10 seconds. The rigorous approach to the analysis of transitional electrons from the case of collisional to collisionless by using kinetic equation is almost impossible. However, it has been shown by Hung and Barnes (1973b) that a mathematical similarity exists between the electron viscous damping and Landau damping as the electrons transition from a collision to a collisionless regime. In other words, the electron viscous damping changes continuously into Landau damping as the ratio of wave frequency to electron collision frequency passes through unity. A similar conclusion was given by Rognlein and Self (1971) based on the hydrodynamic description. Therefore, in the present analysis, the dynamical behavior for the transitional electrons can be described by the fluid-like equations, while the anisotropic ions follow kinetic equations modified by ion-electron collisions.

Before closing this section, let us discuss the validity of the present theory in this transitional region. Assuming that ion and electron temperatures are in the same order, the criteria for the validity of the present theory is

$$\tau_e \leq \left|\frac{1}{\omega}\right| \ll \tau_i \qquad (1)$$

where ω, τ_e and τ_i denote wave frequency, electron and ion collision time,

respectively. There arises a question of whether the fluid-like equations are proper to describe the behavior of electrons under the criteria of validity mentioned in Equation (1). To answer this question, let us look at the conditions for electrons to be able to satisfy the fluid equation. The criteria for electrons to behave like a fluid shall satisfy the following conditions:

$$\tau_e << \left|\frac{1}{\omega}\right| \tag{2a}$$

$$|k_\parallel| a_e \tau_e << 1 \tag{2b}^*$$

where a_e and a_i denote electron and ion thermal speed, respectively, and the subscript $\parallel$ implies the component along the geomagnetic field. In the wave-particle interaction problem, it is generally true that $\omega/k << a_e$ and $\omega/k \geq a_i$. By using this characteristic and the condition (2a), $\tau_e << |1/\omega|$, we may have $|k_\parallel| a_e \sim |\omega|$ and $|k_\parallel| a_e \tau_e \sim |\omega| \tau_e << 1$ when waves propagate fairly near $\pi/2$. Thus, this deduction gives the conclusion which is essentially the criteria (2b). In the limit $|\omega| \tau_e \sim 1$, as pointed out by Barnes (private communications, 1974), the present theory at least gives qualitatively correct results when $|\omega| \tau_e \sim$ a few tenths, and the collisionless theory should be qualitatively correct when $|\omega| \tau_e \geq 3$. Therefore, the similarity between viscous and Landau damping suggests a continuous transition between the two. In this sense, the collisional term is proportional to $\omega\tau_e$, and the Landau damping term is porportional to $\omega (k_\parallel a_e)^{-1}$. Thus, the two terms are always comparable

*The difference in behavior between collisional and collisionless electrons lies in (1) isotropy of electron pressure tensor, (2) the heat equation, (3) the frictional force, and (4) viscosity. Barnes (private communications, 1974) indicated that only the collision time, not the mean free path, is relevant for collisional isotropization; heat conduction along the field lines, which has a scale $1/k_\parallel$ (not $1/k$), is the only appreciable heat transport process; the frictional force (in this case $\propto \nabla_\parallel T_e$) is governed by the length scale $1/k_\parallel$. Thus isotropy, the heat equation, and friction are covered by fluid equations if Equation (2b) is satisfied. Viscosity is more complicated, but the conclusion is the same.

at the time scale of transitional from collisional to collisionless electrons.

As the altitude decreases below the present interest, electron-neutral and ion-neutral collisions become significant, and we have to treat as a three fluid model (e.g. Hung and Wu, 1975).

II-2 Mathematical Formulations

To idealize the problem in hand, we assume that the plasma and magnetic field are, on the average, uniform throughout an effectively infinite volume, that there is no net average electric current, and that the average electron pressure tensor, but not the ion pressure tensor, is isotropic. Let $\underset{\sim}{v}$, P, $\underset{\sim}{q}$ and $\underset{\approx}{\pi}$ denote velocity, pressure, heat flux, and viscous stress tensor respectively and let subscripts or superscripts of e and i denote electrons and ions for the proper situation, respectively. $\underset{\sim}{E}$ and $\underset{\sim}{B}$ represent the electric and magnetic fields, e the ion charge, $m_{(e)}^{(i)}$ the ion or electron mass and c the speed of light. Then the fluid equations for the electrons and the ion velocity distribution f_i may be written as follows (Braginskii, 1965; Hung et al., 1973):

$$\frac{\partial n_e}{\partial t} + \nabla \cdot (n_e \underset{\sim}{v}^e) = 0 \tag{3}$$

$$m_e n_e \frac{d\underset{\sim}{v}_e}{dt} = -\underset{\sim}{\nabla} P_e - \underset{\sim}{\nabla} \cdot \underset{\approx}{\pi}^e - e n_e \left(\underset{\sim}{E} + \frac{1}{c} \underset{\sim}{v}^e \times \underset{\sim}{B}\right) + \underset{\sim}{R}_e \tag{4}$$

$$\frac{3}{2} \cdot n_e \frac{dT_e}{dt} + P_e \underset{\sim}{\nabla} \cdot \underset{\sim}{v}^e = -\underset{\sim}{\nabla} \cdot \underset{\sim}{q}^e - \underset{\approx}{\pi}^e : \underset{\sim}{\nabla}\underset{\sim}{v}^e \tag{5}$$

and

$$\frac{\partial f_i}{\partial t} + \underset{\sim}{v} \cdot \underset{\sim}{\nabla} f_i + \frac{e}{m_i} \left(\underset{\sim}{E} + \frac{1}{c} \underset{\sim}{v} \times \underset{\sim}{B}\right) \cdot \frac{\partial f_i}{\partial \underset{\sim}{v}}$$

$$= \frac{m_e}{m_i \tau_e} \frac{\partial}{\partial \underset{\sim}{v}} \cdot \left(\underset{\sim}{v} f_i + \frac{T_e}{m_i} \frac{\partial f_i}{\partial \underset{\sim}{v}}\right) - \frac{1}{m_i n_i} \underset{\sim}{R}_i \cdot \frac{\partial f_i}{\partial \underset{\sim}{v}} \tag{6}$$

where $P_e = n_e T_e^*$, $p_{(i)}^{i} = n_i T_{(i)}^{i}$, $\frac{d}{dt} = \frac{\partial}{\partial t} + \underset{\sim}{v}_e \cdot \underset{\sim}{\nabla}$, τ_e is the electron collision time, and $\underset{\sim}{R}_e = -\underset{\sim}{R}_i$ is the collisional momentum transfer from ions to

*Here the unit of T is in erg

electron and vise versa. $\underset{\sim}{R}$ is composed of frictional force $\underset{\sim}{R}_U$ and thermal force $\underset{\sim}{R}_T$, $\underset{\sim}{R} = \underset{\sim}{R}_U + \underset{\sim}{R}_T$. The electron thermal flux $\underset{\sim}{q}_e$ is composed of analogous parts, $\underset{\sim}{q}_e = \underset{\sim}{q}_e^U + \underset{\sim}{q}_e^T$. Finally, of course, the electromagnetic fields must satisfy Maxwell's equations.

As it stands, Equations (3) - (5) show the governing equations of electrons, and Equation (6) is the governing equation of ions. Equation (4) includes the collisional momentum transfer from ions to electrons, and we have ignored collisional energy transfer from ions to electrons in Equation (5). This is because the collisional ion-electron energy exchange, whose characteristic time is on the order of or greater than $(m_i/m_e)^{1/2}\,\tau_i$ which is greater than the time scale of present interest, has been neglected. The right-hand side of equation (6) shows the ion-electron collision term which is of the same form as the Fokker-Planck collisional term that describes Brownian motion of particles in a moving medium with temperature T_e. The first term of the collision terms describes the collisional energy transfer from electrons to ions, and the second term implies the collisional momentum transfer from electrons to ions. Again we are going to neglect collisional energy transfer term because the time scale of the collisional energy transfer which affects the evolution of distribution function is on the order of or greater than $\tau_e(m_i/m_e)$ or $\tau_i\,(m_i/m_e)^{1/2}$ that is long compared with the time scale of the problem of current interest.

In the present analysis, we are concerned with waves whose circular frequency ω is small compared with the ion gyrofrequency, and whose wavelengths are long compared with the mean ion Larmor radius. Under such circumstances, the momentum transfer due to collisions can be reduced to (Cf. Hung and Barnes, 1973a; 1973b; 1973c; Hung et al, 1973)

$$\underset{\sim}{R}_e = -0.71\, n_e \nabla_{\parallel} T_e \,. \tag{7}$$

where the subscripts $\parallel, \perp$ refer to the magnetic field direction $\underset{\sim}{e}_z = \underset{\sim}{B}/|\underset{\sim}{B}|$. Similarly, the electron heat flux is

$$\underset{\sim}{q}_e = -K_e \nabla_{\parallel} T_e \tag{8}$$

where K_e is coefficient of electron heat conductivity. Furthermore, under the present condition, the stress tensor becomes (Hung et al, 1973)

$$\pi_{zz}^e = -2\eta_{vo}^e \left[\frac{\partial v_z^e}{\partial z} - \frac{1}{3}\left(\frac{\partial v_x^e}{\partial x} + \frac{\partial v_y^e}{\partial y} + \frac{\partial v_z^e}{\partial z} \right) \right] \qquad (9)$$

$$\pi_{xx}^e = \pi_{yy}^e = -\eta_{vo}^e \left[\frac{\partial v_x^e}{\partial x} + \frac{\partial v_y^e}{\partial y} - \frac{2}{3}\left(\frac{\partial v_x^e}{\partial x} + \frac{\partial v_y^e}{\partial y} + \frac{\partial v_z^e}{\partial z} \right) \right] \qquad (10)$$

$$\pi_{xy}^e \sim \pi_{yx}^e \sim \pi_{xz}^e \sim \pi_{zx}^e \sim \pi_{yz}^e \sim \pi_{zy}^e \sim \mathcal{O}(1/\Omega_e \tau_e)$$

where $\Omega_e = eB/m_e c$ is the electron gyrofrequency, and under the current condition $\Omega_e \tau_e >> 1$.* The zeroth order coefficient of electron viscosity is

$$\eta_{vo}^e = 0.73\, n_e T_e \tau_e \,. \qquad (11)$$

For the ion kinetic equation, the first term on the right-hand-side of Eq. (6) affecting the evolution of the velocity distribution on the time scale is $\sim \tau_e (m_i/m_e)^{1/2}$ which is long compared to time scales of importance for the wave, and may therefore be neglected. Hence, from Eq. (7), the right-hand-side of Eq. (6) is just (Hung et al, 1973)

$$-\frac{1}{m_i n_i} \underset{\sim}{R}_i \cdot \frac{\partial f_i}{\partial \underset{\sim}{v}} = -\frac{0.71}{m_i} (\nabla_{\sim\|} T_e) \cdot \frac{\partial f_i}{\partial \underset{\sim}{v}} \qquad (12)$$

In order to solve Eqs. (3) - (6), we assume $T = \langle T \rangle + \delta T(\underset{\sim}{x}, t)$, $n = \langle n \rangle + \delta n(\underset{\sim}{x}, t)$, $P = \langle P \rangle + \delta P(\underset{\sim}{x}, t)$, $\underset{\sim}{B} = \langle \underset{\sim}{B} \rangle + \delta \underset{\sim}{B}(\underset{\sim}{x}, t)$, $\underset{\sim}{E} = \delta \underset{\sim}{E}(\underset{\sim}{x}, t)$,

*In the ionosphere, the situation is more favorable to this condition as the altitude is higher. In the present case, let us choose the lowest limit of altitude, say 500 Km, $\Omega_e \sim 10^6$ Hz, and $\tau_e \sim 2.5 \times 10^{-3}$. Then, $\Omega_e \tau_e \sim 10^3$ which is much greater than unity. Thus, it can be sure that in the current region of interest, the condition $\Omega_e \tau_e$ is always much greater than unity.

$\underset{\sim}{v}^e = \delta \underset{\sim}{v}^e (\underset{\sim}{x}, t)$ and $f_i = \langle f_i \rangle + \delta f_i (\underset{\sim}{v}, t)$, where $\langle\ \rangle$ denotes ensemble average. We consider the limit of a small amplitude perturbation, $|\delta n/\langle n \rangle| << 1$, etc. If the fluctuations are sinusoidal, the technique of Fourier-Laplace transformation is applicable. Following the calculation procedure of Hung and Barnes (1973a,b) we will be able to obtain velocity fluctuations of ions and electrons in terms of the mobility tensor $\underset{\approx}{M}_j$

$$\delta \underset{\sim}{v}_j = \frac{c}{\langle B \rangle} \underset{\approx}{M}_j \cdot \delta \underset{\sim}{E} \qquad j = e \text{ or } i \tag{13}$$

For the limit of hydromagnetic waves, the displacement current is always negligible. Then the electric current density may be written as

$$\underset{\sim}{j} = - \frac{i\omega}{4\pi} \underset{\approx}{K} \cdot \delta \underset{\sim}{E} \tag{14}$$

where the dielectric tensor is

$$\underset{\approx}{K} = \frac{4\pi i}{\omega} \frac{c}{\langle B \rangle} e \langle n \rangle (\underset{\approx}{M}_i - \underset{\approx}{M}_e) \tag{15}$$

Substituting the mobility tensor $\underset{\approx}{M}_j$ from Eq. (13) in Eq. (15), the explicit form of the dielectric tensor is

$$\underset{\approx}{K} = \begin{bmatrix} K_{xx} & 0 & \mathcal{O}(\omega/\Omega_i) \\ 0 & K_{yy} & K_{yz} \\ \mathcal{O}(\omega/\Omega_i) & K_{zy} & K_{zz} \end{bmatrix} \tag{16}$$

where the components of the dielectric tensor are

$$K_{xx} = -\left(\frac{c}{C_A}\right)^2 \left[\left(\frac{\beta_\perp^i}{\beta_{||}^i} - 1\right) \frac{1}{2y_i^2} - 1\right]$$

$$K_{yy} = -\left(\frac{c}{C_A}\right)^2 \left[\left(\frac{\beta_\perp^i}{\beta_{||}^i} - 1\right)\frac{1}{2y_i^2} - 1 + \frac{k_\perp^2}{k_{||}^2}\,\frac{1}{2y_i^2}\,\frac{\beta_\perp^i}{\beta_{||}^i}\left(2 + \frac{\beta_\perp^i}{\beta_{||}^i}\,Z_i'\right)\right]$$

$$+ i\,\frac{k_\perp^2 a_e^2 \omega_{pe}^2 \zeta_v}{2\omega^2 \Omega_e^2}\left(1 + \frac{2(3\Gamma_e + i2\zeta_v)}{\alpha}\right)$$

$$K_{zz} = -(1-\Lambda)\,\frac{\omega_{pi}^2 Z_i'}{a_{||}^{i\,2} k_{||}^2} + \frac{2\omega_{pe}^2}{a_e^2 k_{||}^2 \alpha}$$

$$K_{yz} = -i\left(\frac{\beta_\perp^i}{\beta_{||}^i}\right)\frac{k_\perp \omega_{pi}^2 Z_i'(1-\Lambda)}{2k_{||}\omega\Omega_i} - i\,\frac{\omega_{pi}^2}{\omega\Omega_i}\,\frac{k_\perp}{k_{||}}\,\frac{3\Gamma_e + i2\zeta_v}{\alpha}$$

$$K_{zy} = i\left(\frac{\beta_\perp^i}{\beta_{||}^i}\right)\frac{k_\perp \omega_{pi}^2 Z_i'}{2k_{||}\omega\Omega_i} + i\,\frac{\omega_{pi}^2}{\omega\Omega_i}\,\frac{k_\perp}{k_{||}}\left(1 + \frac{i6\zeta_v}{\alpha}\right)$$

Here $\omega_{p(i_e)}^2 = 4\pi \langle n_{(i_e)}^i \rangle e^2 / m_{(i_e)}$, $\Gamma_e = 1 + 2/(3 + 2i\eta_{TC})$,
$\eta_{TC} = k_{||}^2 K_e / (\omega \langle n_e \rangle)$, $\alpha = 3(1.71\,\Gamma_e - 0.71) - 4i\,\zeta_v$,
$\zeta_v = 0.73\,\omega\tau_e$, $a_{(\frac{\perp}{||})}^{i\,2} = 2\langle T_{(\frac{\perp}{||})}^i \rangle / m_i$, $a_e^2 = 2\langle T_e \rangle / m_e$,
$\beta_{(\frac{\perp}{||})}^i = 8\pi \langle n \rangle \langle T_{(\frac{\perp}{||})}^i \rangle / \langle B \rangle^2$. $U = \omega / |k_{||}|\,C_A$, $\underset{\sim}{k} = (k_\perp, 0, k_{||})$
$C_A = \langle B \rangle / (4\pi m_i \langle n \rangle)^{1/2}$ Alfven velocity, $y_i = \omega / |k_{||}|\,a_{||}^i$,
$\Lambda = 2.13(\Gamma_e - 1)/\alpha$, and Z_i = $Z(y_i)$ and Z_i' are the plasma dispersion function and its first derivative (Fried and Conte, 1961) respectively.

The requirement that Eq. (14) be consistent with Maxwell's equations gives the dispersion relation

$$\det \left[\left(\frac{c}{\omega}\right)^2 \left(\underset{\sim}{k}\,\underset{\sim}{k} - k^2 \underset{\approx}{1}\right) + \underset{\approx}{K} \right] = 0 \qquad (17)$$

Substituting Eq. (16) in Eq. (17) gives

$$\left[K_{xx} - \left(\frac{c k_{\parallel}}{\omega}\right)^2\right]\left[\left(K_{yy} - \frac{k^2 c^2}{\omega^2}\right)\left(K_{zz} - \frac{k_{\perp}^2 c^2}{\omega^2}\right) - K_{yz}\, K_{zy}\right] = 0 \qquad (18)$$

to lowest order in ω/Ω_i. The first factor is the usual Alfven wave dispersion relation

$$\left(\frac{\omega}{k_{\parallel} C_A}\right)^2 = 1 + \frac{1}{2}\left(\beta_{\perp}^i - \beta_{\parallel}^i\right) \qquad (19)$$

and the second factor, which gives the magneto-acoustic dispersion relation, is

$$\left(K_{yy} - \frac{k^2 c^2}{\omega^2}\right) K_{zz} - K_{zy}\, K_{yz} = 0 \qquad (20)$$

since $|K_{zz}| \gg |k\, c/\omega|^2$.

By using Eq. (16), we can rearrange Eq. (20) by straightforward calculation to give

$$\left[1 + \frac{1}{2}\left(\beta_{\perp}^i - \beta_{\parallel}^i\right) - U^2\right] \cot^2\theta = S\left(U, \omega\tau_e\right) \qquad (21)$$

where

$$-S\left(U, \omega\tau_e\right) = 1 + \beta_{\perp}^i + \frac{1}{2}\frac{\left(\beta_{\perp}^i\right)^2}{\beta_{\parallel}^i} Z_i' - i\frac{\beta_e \zeta_v}{2}\left(1 + \frac{2(3\Gamma_e + i\,2\zeta_v)}{\alpha}\right)$$

$$- \frac{\beta_e \beta_{\parallel}^i}{4\alpha}\frac{\left[\left(\frac{\beta_{\perp}^i}{\beta_{\parallel}^i}\right)\left(\Gamma_e - i\frac{4}{3}\zeta_v\right) Z_i' + 2\left(\Gamma_e + i\frac{2}{3}\zeta_v\right)\right]\left[\alpha\frac{\beta_{\perp}^i}{\beta_{\parallel}^i} Z_i' + 2\left(\alpha + i6\zeta_v\right)\right]}{\beta_e\left(\Gamma_e - i\frac{4}{3}\zeta_v\right) Z_i' - 2\beta_{\parallel}^i} \qquad (22)$$

and $\theta = \measuredangle\left(\underset{\sim}{k}, \langle \underset{\sim}{B} \rangle\right)$, $\beta_e = 8\pi \langle n \rangle \langle T_e \rangle / \langle B \rangle^2$.

II-3 Special Cases of Dispersion Relation

Equation (19) gives the dispersion relation for Alfven waves in a plasma with anisotropic ions. The magneto-acoustic dispersion relation, i.e. Eq. (21), is transcendental and must generally be solved numerically. In order to look at the physics prescribed, it is convenient to consider a few interesting special limits that can provide insight into the character of the waves without laborious calculations.

A. Propagation Parallel to $< \underset{\sim}{B} >$

When $\underset{\sim}{k} \parallel < \underset{\sim}{B} >$, $\cot^2 \theta \to \infty$, so that the left-hand side of Eq. (21) becomes zero, i.e.,

$$\left(\frac{\omega}{k_{\parallel} C_A}\right)^2 = 1 + \frac{1}{2} \left(\beta_{\perp}^i - \beta_{\parallel}^i\right) \tag{23}$$

or $S \to \infty$ (U^2 finite), we find from Eq. (22),

$$Z_i' = \frac{2 < T_{\parallel}^i >}{< T_e >} \quad \frac{1}{\Gamma_e - i \frac{4}{3} \zeta_v} \tag{24}$$

Equation (23) shows that one of the magneto-acoustic modes propagates as an Alfven wave when $\theta = 0$ in a plasma with anisotropic ions. Eq. (24) corresponds to a compressive wave propagating along $< \underset{\sim}{B} >$. The analogous wave in magneto-hydrodynamics is the sound wave, and in a collisionless plasma the analogous wave is the ion acoustic wave which generally undergoes Landau damping (Fried and Conte, 1961).

In the transitional case, the electron collision frequency is on the same order of magnitude as the wave frequency, ζ_v is the order of unity. From the result given by Hung and Barnes (1973b), we found

$$|\eta_{TC}| >> 1 \text{ and } \Gamma_e \approx 1 \tag{25}$$

Under this condition, the dispersion relation can be reduced to (Hung et al., 1973)

$$\left(\frac{\omega}{k}\right)^2 \approx \frac{<T_e>}{m_i} \equiv C_s^2 \tag{26}$$

where C_s denotes ion acoustic velocity, and

$$Im\omega \approx -0.49\,(\omega\tau_e)\,C_s k \tag{27a}$$

or

$$Im\omega \approx -0.67\,\zeta_v\,C_s\,k \tag{27b}$$

Similar to Hung and Barnes (1973b), this result indicates that all ion acoustic waves propagating parallel to the geomagnetic field are Landau-damped, and the damping is weak only if $<T_e> \gg <T_i>$. Particularly, for the case in ionosphere, $<T_e>$ is on the order of $<T_i>$ which implies that most of the ion acoustic mode shall be damped out due to strong Landau damping. Furthermore, Equation (27) also shows that the dissipation rate is proportional to k under the condition when $\omega\tau_e$ is on the order of unity. This result is similar to the collisionless case obtained by Fried and Gould (1961).

For the collisional case, let us consider when $\omega\tau_e$ is the order of (m_e/m_i). The dispersion relation for the weakly damped solution becomes

$$\left(\frac{\omega}{k}\right)^2 = \frac{25 + 4\eta_{TC}^2}{15 + 4\eta_{TC}^2}\,\frac{<T_e>}{m_i} \tag{28}$$

$$\frac{Im\omega}{Re\omega} = -\frac{2\eta_{TC}}{15+4\eta_{TC}^2} \tag{29}$$

To be consistent with the collisional assumption, η_{TC} shall be small compared with unity. Under this assumption, Equations (28) and (29) become

$$\left(\frac{\omega}{k}\right)^2 \approx \frac{5}{3}\,\frac{<T_e>}{m_i} \equiv \frac{5}{3}\,C_s^2 \tag{30}$$

$$Im\omega \approx -0.21\;\tau_e\,a_e^2\,k^2 \tag{31}$$

which is a sonic wave propagating parallel to $<\underset{\sim}{B}>$. Equation (31) shows that the dissipation rate is proportional to k^2 under the condition when $\omega\tau_e$ is on the order of (m_e/m_i). In other words, the dissipational rate obtained from the collisional assumption is equivalent to the collision-dominated case (for example, see Braginskii, 1965). Strictly speaking, under the condition, when $\omega\tau_e$ is on the order of (m_e/m_i), ions are in the transitional from collisional to collisionless, and the arguments similar to Hung and Barnes (1973c) should be employed.

Equations (27) and (31) show that dissipation rate of acoustic modes gradually change from the factor proportional to k^2 to k as the dissipation mechanism transit from Coulomb collisions to Landau damping.

B. Propagation Transverse to $<\underset{\sim}{B}>$

When $\underset{\sim}{k}\perp<\underset{\sim}{B}>$, $Z_i' \to 0$ and $\eta_{TC} \to 0$. Under this condition, Γ_e becomes 5/3 and expression (21) simplifies considerably,

$$\left(\frac{\omega}{k C_A}\right)^2 \simeq 1 + \beta_\perp^i + \beta_e \left[\frac{5}{6} - i\,\frac{\zeta_v}{6}\right] \tag{32}$$

Therefore, we have

$$\left(\frac{\omega}{k}\right)^2 \simeq C_A^2 + \frac{2<T_\perp^i>}{m_i} + \frac{5}{3}\,\frac{<T_e>}{m_i} - i\,\frac{\zeta_v}{3}\,\frac{<T_e>}{m_i} \tag{33}$$

In the transitional case, $\omega\tau_e$ is the order of unity. Equation (33) can be further reduced under the assumption of weakly damped solution, i.e.,

$$\left(\frac{\omega}{k}\right)^2 \approx C_A^2 + \frac{2<T_\perp^i> + \frac{5}{3}\,<T_e>}{m_i}$$

$$= C_A^2 + (a_\perp^i)^2 + \frac{5}{3}\,C_s^2 \tag{34}$$

$$\mathrm{Im}\omega \simeq -0.1216\left(\frac{C_s^2}{\left[C_A^2 + (a_\perp^i)^2 + \frac{5}{3}\,C_s^2\right]^{1/2}}\right)(\omega\tau_e)\,k^2 \tag{35a}$$

or

$$Im\,\omega \simeq -0.0888 \left(\frac{C_s^2\, \zeta_v}{\left[C_A^2 + (a_\perp^i)^2 + \frac{5}{3} C_s^2 \right]^{\frac{1}{2}}} \right) k^2 \qquad (35b)$$

For the collisional case, ζ_v is small as $\omega \tau_e$ is much less than unity. The dissipation rate becomes

$$Im\,\omega \simeq -0.122\, C_s^2\, \tau_e\, k^2 \qquad (36)$$

It is interesting to note that, under present calculation, the phase velocity of the transitional case in Eq. (34) is intermediate between the analogous expression which arises when ions are collisional

$$\left(\frac{\omega}{k}\right)^2 = C_A^2 + \frac{5}{3} \frac{\langle T_i \rangle + \langle T_e \rangle}{m_i} \qquad (37)$$

and that which arises when electrons are collisionless

$$\left(\frac{\omega}{k}\right)^2 = C_A^2 + 2 \frac{\langle T_\perp^i \rangle + \langle T_\perp^e \rangle}{m_i} \qquad (38)$$

In the meanwhile, the dissipation rate also changes from the factor proportional to k^2 to k as the wave particle interaction changes from collisional to transitional cases. In a collisionless plasma, strong Landau damping can occur for θ slightly different from $\pi/2$ (Barnes, 1966). However, when $\underset{\sim}{k}$ is exactly perpendicular to $\langle \underset{\sim}{B} \rangle$, this Landau damping vanishes. In the transitional case, the result is different. No matter how small the electron viscosity is, as long as ζ_v is not zero, viscous dissipation always can be found even when $\underset{\sim}{k}$ is exactly perpendicular to $\langle \underset{\sim}{B} \rangle$.

II-4 Conclusions

In the present study, we have investigated the mechanism of acoustic mode propagation and the characteristics of wave dissipation in the region of the upper atmosphere in which the transport phenomena are transitional from Coulomb collisions to Landau damping. The results from the current analysis are helpful to understand how the acoustic modes propagate and dissipate in the upper atmosphere from ionosphere to magnetosphere, which is significant in the environmental perturbation studies.

As shown in Tables I and II, the present study of acoustic-modes propagation, based on a theoretical model of the upper atmosphere from 500 to 2000 Km altitude, shows that the dissipation rate changes from a factor proportional to the square of the wave vector to a factor only proportional to the wave vector as the altitude becomes higher. These results, approaching the collisional-limited case, are similar to the collision-dominated case (Brapinskii, 1965) in which the dissipation rate is proportional to the square of the wave vector, while the limit approaching the collisionless case is similar to the collisionless case (Fried and Gould, 1961) in which the dissipation rate is proportional to the wave vector. Thus, the dissipation rate changes gradually from a factor proportional to the square of the wave vector to the wave vector as the wave-particle collisions change from collision-dominated to collisionless situations. Physically, the dissipation mechanisms are also different. In the current transition model, acoustic wave dissipation by electrons is through viscous and thermal conduction effects, and by ion particles through Landau damping (wave-particle resonance interactions); while in the collision-dominated case, it is simply due to viscous and thermal conduction effects, and in the

collision-free case it is due to Landau damping. For the waves propagating along the magnetic field, two extreme examples are given for the transitional model, namely the collisional-limited case with $\omega\tau_e$ on the order of (m_e/m_i) and the transitional-limited case with $\omega\tau_e$ on the order of unity. The collisional-limited case of the transitional model shows that the square of the characteristic phase velocity of acoustic waves in square of ion acoustic velocity multiplied by 5/3 or γ (where γ is the ratio of constant pressure specific heat to constant volume specific heat) which looks quite similar to the collision-dominated model in which square of the phase velocity is the square of ordinary sound wave speed, $\gamma P/\rho$ (where $\rho = m_e n_e + m_i n_i + m_n n_n$). In the transitional-limited case of transitional model phase velocity is equivalent to ion acoustic velocity which is exactly corresponding to the phase velocity in collisionless case. In other words, change of the phase velocity of acoustic modes from collisional to collisionless cases are from a factor of γ or $\frac{5}{3}$ to a factor of unity. Thus, it is expected that the phase velocity of acoustic wave decreases gradually from collisional to collisionless cases if the temperature keeps a constant value. Similar results are also shown for waves propagating transverse to magnetic field.

Finally, we may conclude from these studies that the long wavelength acoustic mode is a much less damped wave for the collisional than the collisionless cases, and the short wavelength acoustic mode is more easily observable in the collisionless than in the collisional cases since the dissipation rate of the acoustic mode changes from a factor proportional to the square of the wave vector to the wave vector as the altitude increases in the transitional region of the ionosphere. In the meantime, the physical mechanisms and phase velocities are also different for collision-dominated transitional and collisionless cases.

Table I. Comparisons of the Propagation of Acoustic Modes in Collision-Dominated, Transitional and Collisionless Media Along Magnetic Field

	Collision-Dominated	Transitional		Collisionless
		$\omega \tau_e \sim \mathcal{O}\left(\frac{m_e}{m_i}\right)$	$\omega \tau_e \sim \mathcal{O}(1)$	
Phase Velocity	$\left(\frac{\gamma p}{\rho}\right)^{1/2}$	$\left(\frac{5}{3} c_s^2\right)^{1/2}$	c_s	c_s
Dissipation Rate	Proportional to $\underset{\sim}{k}^2$	Proportional to $\underset{\sim}{k}^2$	Porportional to $\underset{\sim}{k}$	Proportional to $\underset{\sim}{k}$
Dissipation Mechanism	Viscous and Thermal Conduction	Electrons — Viscous and Thermal Conduction Ions — Landau Damping		Landau Damping

Table II. Comparisons of the Propagation of Acoustic Modes in Collision-Dominated, Transitional and Collisionless Media Transverse to Magnetic Field

	Collision Dominated	Transitional		Collisionless
		$\omega T_e \sim \mathcal{O}\left(\frac{m_e}{m_i}\right)$	$\omega T_e \sim \mathcal{O}(1)$	
Phase Velocity	$\left(C_A^2 + \frac{5}{3}\frac{\langle T_i\rangle + \langle T_e\rangle}{m_i}\right)^{1/2}$	$\left(C_A^2 + \frac{2\langle T_\perp^i\rangle + \frac{5}{3}\langle T_e\rangle}{m_i}\right)^{1/2}$		$\left(C_A^2 + 2\frac{\langle T_\perp^i\rangle + \langle T_\perp^e\rangle}{m_i}\right)^{1/2}$
Dissipation Rate	Proportional to $\underset{\sim}{k}^2$	Proportional to $\underset{\sim}{k}^2$		Vanish
Dissipation Mechanism	Viscous and Thermal Conduction	Electrons — Viscous and Thermal Conduction Ions — Landau Damping Vanishes at $\underset{\sim}{k} \perp \langle \underset{\sim}{B} \rangle$		Landau Damping Vanishes at $\underset{\sim}{k} \perp \langle \underset{\sim}{B} \rangle$

References

Barnes, A., Collisionless Damping of Hydromagnetic Waves, Phys. Fluids, 1, 1483, 1966.

Barnes, A. (Private Communication) 1974.

Bernstein, I.B., and S. K. Trehan, Plasma Oscillations, Nuclear Fusion 1, 3, 1960.

Bhatnagar, P. L., E. P. Gross and M. Krook, A Model for Collision Processes in Gases. I. Small Amplitude Processes in Charged and Neutral One-Component Systems, Phys. Rev. 94, 511, 1954.

Braginskii, S. I., Transport Processes in a Plasma, in Reviews of Plasma Physics, Vol. 1, edited by M. A. Leontovich, p. 205, Consultant Bureau, New York, 1965.

Chapman, S., and T. G. Cowling, The Mathematical Theory of Non-uniform Gases, University Press, Cambridge, 1960.

Fried, B. D., and S. D. Conte, The Plasma Dispersion Function, Academic Press, New York, 1961.

Fried, B. D., and R. W. Gould, Longitudinal Ion Oscillations in a Hot Plasma, Phys. Fluids 4, 139, 1961.

Gross, E. P., and M. Krook, Model for Collision Processes in Gases: Small-Amplitude Oscillations of Charged Two-Component Systems, Phys. Rev. 102, 593, 1956.

Hamel, B. B., Kinetic Model for Binary Gas Mixtures, Phys. Fluids 8, 418, 1965.

Hanson, W. B., Satellite Environment Handbook, edited by F. S. Johnson, Stanford University Press, Stanford, California, 1965.

Holway, L. H., Jr., New Statistical Models for Kinetic Theory: Methods of Construction, Phys. Fluids 9, 1958, 1966.

Hung, R. J., and A. Barnes, Dissipation of Hydromagnetic Waves with Application to the Outer Solar Corona, I. Collisionless Protons and Collisional Electrons, Astrophys. J. 180, 253, 1973a.

Hung, R. J., and A. Barnes, Dissipation of Hydromagnetic Waves with Application to the Outer Solar Corona, II. Transition from Collisional to Collisionless Electrons, Astrophys. J., 180, 271, 1973b.

Hung, R. J., and A. Barnes, Dissipation of Hydromagnetic Waves with Application to the Outer Solar Corona, III. Transition from Collisional to Collisionless Protons, Astrophys. J., 181, 183, 1973b.

Hung, R. J., S. T. Wu, and R. E. Smith, Propagation of Hydromagnetic Waves in Upper F2 Region, Planet. Space Sci., 21, 2157, 1973.

Hung, R. J. and S. T. Wu, Cross Field Plasma Drift Instabilities and Equatorial Sporadic E, 1975 (in preparation).

Rognlien, T. D., and S. A. Self, An Acoustic Instability at Two-temperature, Collisional, Fully Ionized Plasma, Phys. Rev. Lett., 27, 792, 1971.

Tolstoy, I., Damping of Very Long Internal Gravity Waves in the Atmosphere, AFOSR-TR-72-0085 (or AD 735386) National Technical Information Service, Springfield, Va., 22151, 1972.

CHAPTER III
THREE FLUIDS DESCRIPTION OF THE CROSS FIELD PLASMA DRIFT INSTABILITIES AND EQUATORIAL SPORADIC E*

III-1 General Statement of the Problem

Triggering mechanisms of sporadic E, in general, depend on the geomagnetic latitudinal location. For example, sporadic E in the high latitude region and the impinging of energetic particles through magnetospheric cleft, is considered to be responsible for the mechanism. In the middle latitude, it is believed that the redistribution of ionized particles caused by the wind shear may be responsible for the creation of sporadic E. Concerning the equatorial region, Matsushita (1951), suggested that the equatorial sporadic E (Es-q) can be related to the equatorial electrojet. Since then, intense study of the irregularities of equatorial electrojet has been carried out by employing the Jicamarca VHF radar echoes. In the present study, our interest is mainly limited to the case where the sporadic E occurs near the geomagnetic equator.

The equatorial electrojet is a strong current embedded in a slightly ionized ionospheric plasma in the E layer near the geomagnetic equator. This current is a flow of electrons, motivated by $\underset{\sim}{E}_z \times \underset{\sim}{B}$ drift, across geomagnetic field lines through ions and neutrals, where $\underset{\sim}{E}_z$ is the induced electric field along vertical height and $\underset{\sim}{B}$ is the geomagnetic field. By using radar backscatter, extensive investigations have made it possible to elucidate physical processes for the formation and movement of irregularities. Balsley (1965; 1969a, b) classified the

*Part of the results are published in the Proceedings of International Conference on Recent Advances in the Physics and Chemistry of the E Region (Ed. by S. Matsushita and L. G. Smith) August 1974.

irregularities into types I and II. The instabilities driven by the electrons drifting through ions across the magnetic field that was proposed by Farley (1963a, b) and Buneman (1963) are generally accepted as the generation mechanism of this type I irregularities. Type II irregularities are considered to be generated by a plasma density gradient in crossed electric and magnetic fields.

The analysis of VHF radar echoes from electron concentration irregularities in the equatorial electrojet by Balsley (1969a) has indicated that there are two distinct types of irregularities in the region. Also, Cohen (1973), by using the spectral decomposition of the power spectrum of radar echoes at 50 MHz from the equatorial electrojet, found out that the phase velocity of type I irregularities is comparable to the ion-acoustic speed, and the electron drift velocity can exceed the ion-acoustic speed. The indication of experimental results that the electron drift velocity in the equatorial electrojet can be supersonic is contrary to some existing theoretical opinions (e.g., Sato, 1973). For the type II irregularities, the experimental results showed that both phase velocity of irregularities and electron drift velocity are smaller than the ion-acoustic speed.

The theoretical treatment of the problem of growth of type I and type II irregularities in the electrojet has been examined extensively by Rogister (1971, 1972), Rogister and d'Angelo (1970), and Sudan, et al. (1973). However, their theoretical models were limited to the two fluid model (i.e., ion and electron fluid) and no neutral interaction was considered. Furthermore, they did not cooperate the energy transport in their studies and treated only the problems of the density gradients in their models. The problem of temperature gradients was considered by Cunnold (1972). However, he also used the two-fluid approach and did

not consider convective motions for both ions and electrons. In the present study, we propose an inhomogeneous three fluid model to investigate the unified theory of type I and II electrojet irregularities which may be relevant to the mechanism of equatorial sporadic E. Particularly, we are interested in physical mechanisms of type I and type II irregularities and how the electron particles are accelerated due to $E_z \times B$ drift in the electrojet. Thus, we have examined the density gradients and temperature gradients for three species and both as the driven mechanism for the electrojet. The results of computer computations based on the present model have been compared to the experimental observations with reasonably good agreements.

III-2 Mathematical Formulations

This study is concerned with the propagation of ionospheric disturbances through the inhomogeneous medium which includes the species of electron, ion and neutral particles. Thus, a three-fluid model is proposed to investigate the characteristics and instabilities of the propagation of waves and particles.

Let n, $\underset{\sim}{v}$, T, P and ν denote number density, velocity, temperature, pressure and collision frequency, respectively, and let superscripts and subscripts e, i and n denote electrons, ions and neutral species, respectively. Let $\underset{\sim}{E}$ and $\underset{\sim}{B}$ be the electric and magnetic fields, e the ion charge, m the mass, and c the speed of light. Then the governing equations of particles and fields may be written as follows:

$$\frac{\partial n_j}{\partial t} + \underset{\sim}{\nabla} \cdot (n_j \underset{\sim}{v}_j) = 0 \qquad j = e, i \text{ and } n \tag{1}$$

$$m_n n_n \frac{d\underset{\sim}{v}_n}{dt} = - \underset{\sim}{\nabla} P_n - m_n n_n \nu_{ni} (\underset{\sim}{v}_n - \underset{\sim}{v}_i) \tag{2}$$

$$m_e n_e \frac{d\underset{\sim}{v}_e}{dt} = - \underset{\sim}{\nabla} P_e - e n_e \left(\underset{\sim}{E} + \frac{1}{c} \underset{\sim}{v}_e \times \underset{\sim}{B}\right) - m_e n_e \nu_{ei} (\underset{\sim}{v}_e - \underset{\sim}{v}_i) - m_e n_e \nu_{en} (\underset{\sim}{v}_e - \underset{\sim}{v}_n) \tag{3}$$

$$m_i n_i \frac{d\underset{\sim}{v}_i}{dt} = - \underset{\sim}{\nabla} P_i + e n_i \left(\underset{\sim}{E} + \frac{1}{c} \underset{\sim}{v}_i \times \underset{\sim}{B}\right) - m_i n_i \nu_{ie} (\underset{\sim}{v}_i - \underset{\sim}{v}_e) - m_i n_i \nu_{in} (\underset{\sim}{v}_i - \underset{\sim}{v}_n) \tag{4}$$

$$\frac{3}{2} n_j \frac{dT_j}{dt} + P_j \underset{\sim}{\nabla} \cdot \underset{\sim}{v}_i = 0 \qquad \text{with } j = e, i \text{ and } n \tag{5}$$

where $d/dt = \partial/\partial t + (\underset{\sim}{v}\cdot\underset{\sim}{\nabla})$. Finally, of course, the electromagnetic fields must satisfy Maxwell's equations.

In the present study, the time scale of interest is on the order of 0.1 second. Under this condition, momentum exchange through particle collisions between neutral-ion, electron-neutral, electron-ion, ion-neutral, and ion-electron, but not neutral-electron, plays the significant role in our analysis. Energy exchange through collision has been ignored in the present model because the time scale of interest of energy exchange through collisions is much longer than the time scale of interest in the present study.

In general, physical parameters in the upper atmosphere are inhomogeneous. Particularly, the inhomogeneities of number densities and temperatures for three species of particles along the vertical height is significant. As shown in Figure 1, we choose a Cartesian coordinate system as a geometry for the magnetic equator, where $\underset{\sim}{e}_z$ is vertically upward, $\underset{\sim}{e}_x$ is eastward, and $\underset{\sim}{e}_y$ is northward. The inhomogeneities of number densities and temperatures are assumed to be much smaller than their average values respectively so that Taylor series expansion with respect to the inhomogeneity is applicable (Mikhailovskii, 1967; Hung and Liu, 1971), i.e.,

$$n_j = \langle n_j \rangle (1 + \underset{\sim}{k}^*_{nj} \cdot d\underset{\sim}{z}) + \delta n_j \tag{6}$$

$$T_j = \langle T_j \rangle (1 + \underset{\sim}{k}^*_{Tj} \cdot d\underset{\sim}{z}) + \delta T_j \qquad \text{with } j = e, i \text{ and } n \tag{7}$$

where

$$\underset{\sim}{k}^{*}_{nj} = \frac{1}{\langle n_j \rangle} \left.\frac{d\langle n_j \rangle}{d\underset{\sim}{z}}\right]_{z = z_o} , \quad \underset{\sim}{k}^{*}_{Tj} = \frac{1}{\langle T_j \rangle} \left.\frac{d\langle T_j \rangle}{d\underset{\sim}{z}}\right]_{z = z_o}$$

and $\langle\ \rangle$ the average value and δ the small fluctuation of physical parameters.

The limit of small amplitude fluctuations, $|\delta n/\langle n \rangle| << 1$, etc., is considered for the calculation of dispersion relation. If the fluctuations are sinusoidal, i.e., proportional to

$$\exp\left[i\ (\underset{\sim}{k} \cdot \underset{\sim}{x} - \omega t)\right]$$

equations (1) - (5) become, after substituting equations (6) - (7) and linearization,

$$\frac{\delta n_j}{\langle n_j \rangle} = \frac{1}{\omega}\ (\underset{\sim}{k} + i\ \underset{\sim}{k}^{*}_{nj}) \cdot \delta\underset{\sim}{v}_j \qquad j = e,\ i \text{ and } n \tag{8}$$

$$\delta\underset{\sim}{v}_n\ (1 + i\ \frac{\nu_{ni}}{\omega}) = \frac{2a_n^2}{5\omega^2}\ [(\underset{\sim}{k} - i\ \frac{3}{2}\ \underset{\sim}{k}^{*}_{Tn}) \cdot \delta\underset{\sim}{v}_n]\ (i\ \underset{\sim}{k}^{*}_{nn} + \underset{\sim}{k})$$

$$- \frac{3a_n^2}{5\omega^2}\ [(\underset{\sim}{k} + i\ \underset{\sim}{k}^{*}_{nn}) \cdot \delta\underset{\sim}{v}_n]\ (i\ \underset{\sim}{k}^{*}_{Tn} - \underset{\sim}{k})$$

$$+ i\ \frac{\nu_{ni}}{\omega}\ \delta\underset{\sim}{v}_i \tag{9}$$

$$\delta\underset{\sim}{v}_i\ \left(\frac{\omega}{\Omega_i} + i\ \frac{\nu_{in}}{\Omega_i}\right) = \frac{3a_i^2}{5\Omega_i}\ \left\{\left[\frac{2}{3\omega}\ (\underset{\sim}{k} - i\ \frac{3}{2}\ \underset{\sim}{k}^{*}_{Ti}) \cdot \delta\underset{\sim}{v}_i\right]\ (\underset{\sim}{k} + i\ \underset{\sim}{k}^{*}_{ni})\right.$$

$$\left. + \left[\frac{1}{\omega}\ (\underset{\sim}{k} + i\ \underset{\sim}{k}^{*}_{ni}) \cdot \delta\underset{\sim}{v}_i\right]\ (\underset{\sim}{k} - i\ \underset{\sim}{k}^{*}_{Ti})\right\} + i\ \frac{c}{\langle B \rangle}\ \delta\underset{\sim}{E}$$

$$+ i\ \delta\underset{\sim}{v}_i \times \underset{\sim}{e}_y + i\ \frac{\nu_{in}}{\Omega_i}\ \delta\underset{\sim}{v}_n \tag{10}$$

$$\frac{3a_e^2}{5\Omega_e}\left[(\underset{\sim}{k}+i\,\underset{\sim}{k}^*_{ne})\frac{\delta T_e}{\langle T_e\rangle}+(\underset{\sim}{k}-i\,\underset{\sim}{k}^*_{Te})\frac{\delta n_e}{\langle n_e\rangle}\right]-i\frac{c}{\langle B\rangle}\,\delta\underset{\sim}{E}$$

$$-i\,\delta\underset{\sim}{v}_e\times\underset{\sim}{e}_y-i\frac{\nu_{en}}{\Omega_e}(\delta\underset{\sim}{v}_e-\delta\underset{\sim}{v}_n)-i\frac{\nu_{ei}}{\Omega_e}(\delta\underset{\sim}{v}_e-\delta\underset{\sim}{v}_i)=0 \qquad (11)$$

and

$$\frac{\delta T_j}{\langle T_j\rangle}=\frac{2}{3\omega}(\underset{\sim}{k}-i\,\frac{3}{2}\,\underset{\sim}{k}^*_{Tj})\cdot\delta\underset{\sim}{v}_j \qquad j=e,\ i \text{ and } n \qquad (12)$$

where $\underset{\sim}{e}_y$ is a unit vector in y-direction, which is along geomagnetic north, $a_j^2=(5/3)\langle T_j\rangle/m_j$ is the square of sound speed of species j, and $\Omega_j=eB/m_jc$ is the cyclotron frequency of species j.

By using equations (8) - (12) together with Maxwell's equations, we can obtain the following solutions:

$$\begin{bmatrix}\delta v_n^x\\ \delta v_n^y\\ \delta v_n^z\end{bmatrix}=\begin{bmatrix}\xi_n^x & \xi_n^y & \xi_n^z\\ \eta_n^x & \eta_n^y & \eta_n^z\\ \zeta_n^x & \zeta_n^y & \zeta_n^z\end{bmatrix}\begin{bmatrix}\delta v_i^x\\ \delta v_i^y\\ \delta v_i^z\end{bmatrix} \qquad (13)$$

$$\begin{bmatrix}\delta v_i^x\\ \delta v_i^y\\ \delta v_i^z\end{bmatrix}=\frac{c}{\langle B\rangle}\begin{bmatrix}\xi_i^x & \xi_i^y & \xi_i^z\\ \eta_i^x & \eta_i^y & \eta_i^z\\ \zeta_i^x & \zeta_i^y & \zeta_i^z\end{bmatrix}\begin{bmatrix}\delta E_x\\ \delta E_y\\ \delta E_z\end{bmatrix} \qquad (14)$$

and

$$\begin{bmatrix} \delta v_e^x \\ \delta v_e^y \\ \delta v_e^z \end{bmatrix} = \frac{c}{\langle B \rangle} \begin{bmatrix} \xi_e^x & \xi_e^y & \xi_e^z \\ \eta_e^x & \eta_e^y & \eta_e^z \\ \zeta_e^x & \zeta_e^y & \zeta_e^z \end{bmatrix} \begin{bmatrix} \delta E_x \\ \delta E_y \\ \delta E_z \end{bmatrix} \qquad (15)$$

The expressions of ξ_y^x, ξ_j^y, ξ_j^z, η_j^x, η_j^y, η_j^z, ζ_j^x, ζ_j^y, and ζ_j^z are very complicated, therefore, we will skip these results given by Hunt (1974).

It is very interesting to point out that the neutral wind is mainly induced by the ion motion through ion-neutral collisions as shown in equation (13). If we substitute equation (14) in equation (13), we have

$$\begin{bmatrix} \delta v_n^x \\ \delta v_n^y \\ \delta v_n^z \end{bmatrix} = \frac{c}{\langle B \rangle} \begin{bmatrix} M_{xx}^n & M_{xy}^n & M_{xz}^n \\ M_{yx}^n & M_{yy}^n & M_{yz}^n \\ M_{zx}^n & M_{zy}^n & M_{zz}^n \end{bmatrix} \begin{bmatrix} \delta E_x \\ \delta E_y \\ \delta E_z \end{bmatrix} \qquad (16)$$

where

$$M_{xx}^n = \xi_n^x \, \xi_i^x + \xi_n^y \, \eta_i^x + \xi_n^z \, \zeta_i^x$$

$$M_{xy}^n = \xi_n^x \, \xi_i^y + \xi_n^y \, \eta_i^y + \xi_n^z \, \zeta_i^y$$

$$M_{xz}^n = \xi_n^x \, \xi_i^z + \xi_n^y \, \eta_i^z + \xi_n^z \, \zeta_i^z$$

$$M_{yx}^n = \eta_n^x \, \xi_i^x + \eta_n^y \, \eta_i^x + \eta_n^z \, \zeta_i^x$$

$$M^n_{yy} = \eta^x_n \; \xi^y_i + \eta^y_n \; \eta^y_i + \eta^z_n \; \zeta^y_i$$

$$M^n_{zy} = \eta^x_n \; \xi^z_i + \eta^y_n \; \eta^z_i + \eta^z_n \; \zeta^z_i$$

$$M^n_{zx} = \zeta^x_n \; \xi^x_i + \zeta^y_n \; \eta^x_i + \zeta^z_n \; \zeta^x_i$$

$$M^n_{zy} = \zeta^x_n \; \xi^y_i + \zeta^y_n \; \eta^y_i + \zeta^z_n \; \zeta^y_i$$

$$M^n_{zz} = \zeta^x_n \; \xi^z_i + \zeta^y_n \; \eta^z_i + \zeta^z_n \; \zeta^z_i$$

Equation (16) shows how neutral wind is accelerated by the electromagnetic fields through ion-neutral collisions.

Now the electric current density, δj, electric conductivity tensor, Kapa $\underset{\sim}{\sigma}$, and dielectric tensor, $\underset{\approx}{K}$, are defined as

$$\delta \underset{\sim}{j} = e \langle n \rangle \; (\delta \underset{\sim}{v}_i - \delta \underset{\sim}{v}_e) \tag{17}$$

$$\delta j_\alpha = \sigma_{\alpha\beta} \; \delta E_\beta \tag{18}$$

and

$$K_{\alpha\beta} = \delta_{\alpha\beta} + i \, \frac{4\pi}{\omega} \, \sigma_{\alpha\beta} \tag{19}$$

By substituting equations (14), (15), (17), and (18) in equation (19), we have the expression of dielectric tensor $K_{\alpha\beta}$ which characterizes the material constant of ionosphere, i.e.,

$$\underset{\approx}{K} = \begin{bmatrix} 1 & 0 & 0 \\ 0 & 1 & 0 \\ 0 & 0 & 0 \end{bmatrix} + i \, \frac{\omega^2_{pe}}{\omega \Omega_e} \begin{bmatrix} \xi^x_i - \xi^x_e & \xi^y_i - \xi^y_e & \xi^z_i - \xi^z_e \\ \eta^x_i - \eta^x_e & \eta^y_i - \eta^y_e & \eta^z_i - \eta^z_e \\ \zeta^x_i - \zeta^x_e & \zeta^y_i - \zeta^y_e & \zeta^z_i - \zeta^z_e \end{bmatrix} \tag{20}$$

where $\omega_{pe}^2 = 4\pi \langle n \rangle \ e^2/m_e$.

As is well known, the requirement that equation (20) be consistent with Maxwell's equations gives the dispersion relation

$$\det \left[\left(\frac{c}{\omega}\right)^2 \left(\underset{\sim}{k}\ \underset{\sim}{k} - k^2 \underset{\sim}{1} \right) + \underset{\approx}{K} \right] = 0 \qquad (21)$$

The dispersion relation which governs the behavior of wave-like disturbances in the ionosphere is quite complicated. The numerical computation is generally requested to solve this problem.

III-3 Preliminary Results of Numerical Computation and Conclusions

As mentioned earlier, the purpose of the present study is to investigate the plasma drift instabilities in which the growing drift waves propagating across the field lines may contribute to the triggering mechanism of sporadic E in the region of magnetic equator. Since the dynamics of wave propagation is solely governed by the dispersion relation, equation (21) which is quite complicated, the numerical computation is a necessity to the present investigation.

At an altitude of 110 Km, the parameters with $T_e \simeq T_i \simeq T_n = 250°K$, $\nu_{en} = 2.88 \times 10^4\ sec^{-1}$, $\nu_{in} = 8.9 \times 10^2\ sec^{-1}$, $\nu_{ei} = 1.8 \times 10^2\ sec^{-1}$, $\nu_{ne} = 8.9 \times 10^{-4} sec^{-1}$, $\nu_{ni} = 3.2 \times 10^{-5}\ sec^{-1}$, and $\Omega_i = 1.5 \times 10^2\ sec^{-1}$ are chosen. All the other values of physical parameters under non-disturbed conditions are chosen from U. S. Standard Atmosphere (1962, 1966). In order to have a better comparison with existing models of type I and type II irregularities, calculations are proceeded in the following three cases:

(1) Case A: Electrojet Without Density Gradients

In this case, we assume that $k^*_{nj} \to 0$ and $k^*_{Tj} \neq 0$. The date of temperature gradients for three species are chosen from U. S. Standard Atmosphere (1962, 1966). Three roots with positive growth rate were obtained for this case from dispersion relation (eq. 21). Table I shows the result of this case. Westward drift waves with phase velocities from 303 m/sec to 384 m/sec are excited. Growth rates of the excited waves ($Im\,\omega/Re\omega$) range from 0.06 to 0.17. This

kind of instability resembles type I irregularities.

(2) Case B: Electrojet Without Temperature Gradients

In this case, we assume that $k^*_{Tj} \to 0$ and $k^*_{nj} \neq 0$. Again the data of density gradients for three species are chosen from U. S. Standard Atmosphere (1962, 1966). Four roots with positive growth rate were obtained for this case from dispersion relation (eq. 21). Table 2 indicates this result. Again westward drift waves with phase velocities from 329 m/sec to 395 m/sec are excited. Growth rates of the excited waves ($Im\omega/Re\omega$) range from 0.04 to 0.12. Similar to Case A, this kind of instability resembles type I irregularities.

(3) Case C: Electrojet With Density and Temperature Gradients

In this case, both $k^*_{Tj} \neq 0$ and $k^*_{nj} \neq 0$. Again data for both temperature and density gradients for three species are chosen from U. S. Standard Atmosphere (1962, 1966). Nine roots with positive growth rate were obtained from dispersion relation (eq. 21) for this case. Table 3 shows this result. Westward drift waves with phase velocities from 180 m/sec to 307 m/sec are excited. In this case, none of the waves, which propagate faster than ion acoustic speed, are excited. Growth rates of the excited waves are generally very high, ranging from 1 to 3. This instability resembles type II irregularities.

Comparing the results in Tables 1 to 3, some interesting points are discovered. Type I irregularities of equatorial electrojet in our model can be generated in the inhomogeneous medium along the vertical height if either the temperature gradient or density gradient vanishes. In the meanwhile, type II irregularities can be excited if neither the temperature gradient nor the density gradient vanishes. Furthermore, the growth rate of irregularities obtained from the calculation suggests that the wave-wave nonlinear interaction should be taken into account for type II irregularities while it may be proper to proceed linearized theory for type I irregularities. In other words, turbulent mechanism, which is different from the present model, may be the characteristic of type II irregularities, while the laminar theory is applicable to type I irregularities.

Sugiura and Poros (1969) suggested that the motion of east-west electron electrojet drift velocity δv_e^x can be determined as

$$\delta v_e^x = \frac{c}{\langle B \rangle} \delta E_z \ (z). \tag{22}$$

In our expression, ξ_e^x and ξ_e^y, in equation (15), are practically ıible since ξ_e^x and ξ_e^y are several orders smaller than ξ_e^z. Therefore, we have

$$\delta v_e^x = \frac{c}{\langle B \rangle} \xi_e^z \ \delta E_z \ (z). \tag{23}$$

In our case, numerical computation shows that ξ_e^z is practically on the order of unity which also agrees with equation (22). Since the vertical polarization field varies from 20 mV/m in the daytime to -20mV/m at night (Kato, 1973; Lee and Kennel, 1973), change of direction of electron drift in the equatorial electrojet from westward during daytime to eastward during night hours can be fully explained based on this mechanism.

To check the observations made by Cohen (1973) that the horizontal electron velocity in the equatorial electrojet may exceed the ion acoustic speed, numerical computations are also made by employing equation (15) to calculate the westward electron velocity in the electrojet for the type I irregularities. The results show that the westward velocity of electrons may reach 450 m/sec, which exceeds the ion acoustic speed, for vertical polarization electric field being 18 mV/m and westward polarization electric field being -1 mV/m. This result agrees with the experimental observations made by Cohen (1973).

In closing, the following conclusions are made from the present study: (1) triggering mechanism for the sporadic E near magnetic equator is due to the inhomogeneous medium (gradients of densities and temperatures in three species of particles along the vertical height) which create cross-field plasma irregularities imposed on westward electrojet; (2) type I irregularities of equatorial electrojet can be excited in the inhomogeneous medium along the vertical height if either the temperature gradient or density gradient of three species of particles vanishes; (3) type II irregularities of electrojet can be excited for the existence of both temperature and density gradients of three species along vertical height; (4) strong growth rate of type II irregularities suggests that turbulent mechanism may be the main structure for the type II irregularities; (5) rather weak growth rate in type I irregularities indicates that linearized theory may be applicable for type I irregularities; (6) vertical polarization field which shifts from positive in daytime to negative at night indicates horizontal electron drift in electrojet change from westward in daytime

to eastward at night; (7) the westward electron drift velocity in electrojet can be on the order of or exceeds ion acoustic speed for type I irregularities.

Finally, we have shown that the three-fluid model can be used to predict both type I and type II irregularities by introducing proper physical mechanisms; namely, density gradients and temperature gradients of the three species.

REFERENCES

Balsley, B. B. (1965), "Some Additional Features of Radar Returns from the Equatorial Electrojet," J. Geophys. Res. 70, 3175-3182.

Balsley, B. B. (1969a), "Some Characteristics of Non-Two-Stream Irregularities in the Equatorial Electrojet," J. Geophys. Res. 74, 2333-2347.

Balsley, B. B. (1969b), "Measurement of Electron Drift Velocities in the Night-Time Equatorial Electrojet," J. Atmos. Terr. Phys. 31, 475-478.

Buneman, O. (1963), "Excitation of Field Aligned Sound Waves by Electron Streams," Phys. Rev. Lett. 10, 285.

Cohen, R. (1973), "Phase Velocities of Irregularities in the Equatorial Electrojet," J. Geophys. Res. 78, 2222-2231.

Cunnold, D. M. (1972), "An Electron Temperature Gradient Instability and Its Possible Application to the Ionosphere, J. Geophys. Res., 77, 223-233.

Farley, D. T. (1963a), Two-Stream Plasma Instability as a Source of Irregularities in the Ionosphere," Phys. Rev. Lett. 10, 279.

Farley, D. T. (1963b), "A Plasma Instability Resulting in Field-Aligned Irregularities in the Ionosphere," J. Geophys. Res. 68, 6083.

Hung, R. J. and V. C. Liu (1971), "Effect of Temperature Gradient on the Drift Instabilities in a High-β Collisionless Plasma," Phys. Fluids 14, 2061-2063.

Hung, R. J. (1974), "Dynamics of ULF Waves in the Magnetosphere," Research Report, University of Alabama in Huntsville.

Kato, S. (1973), "Movement of Irregularities in the Equatorial E-Region - A Review," J. Atmos. Terr. Phys. 35, 1073-1082.

Lee, K., and C. F. Kennell (1973), "Convective Amplification of Type I Irregularities in the Equatorial Electrojet," J. Geophys. Res. 78, 4619-4629.

Matsushita, S. (1951), "Intense E_s Ionization Near the Magnetic Equator," J. Geomagn. Geoelect. 3, 44-46.

Mikhailovskii, A. B. (1967), in Reviews of Plasma Physics, Vol. 3, (ed. by M. A. Leontovich), Consultants Bureau, New York.

Rogister, Andre (1971), "Nonlinear Theory of Type I Irregularities in the Equatorial Electrojet," J. Geophys. Res., 76, 7754-7760.

Rogister, Andre (1972), "Nonlinear Theory of Cross Field Instability With Application to the Equatorial Electrojet," J. Geophys. Res., 79, 2975-2981.

Rogister, A. and N. D'Angelo (1970), "Type II Irregularities in the Equatorial Electrojet, " J. Geophys. Res., 75, 3879-3887.

Sato, T. (1973), "Unified Theory of Type I and II Irregularities in the Equatorial Electrojet," J. Geophys. Res., 78, 2232-2243.

Sundan, R. N., J. Akinrimisi and D. T. Farley (1973), "Generation of Small-Scale Irregularities in the Equatorial Electrojet," J. Geophys. Res., 78, 240-248.

Sugiura, M. and D. J. Poros (1969), "An Important Model Equatorial Electrojet With a Meridional Current System," J. Geophys. Res., 74, 4025-4034.

U. S. Standard Atmosphere (1962).

U. S. Standard Atmosphere (1966).

FIGURE CAPTION

Figure 1 Geometry of Cartesian Coordinate System Near Geomagnetic Equator.

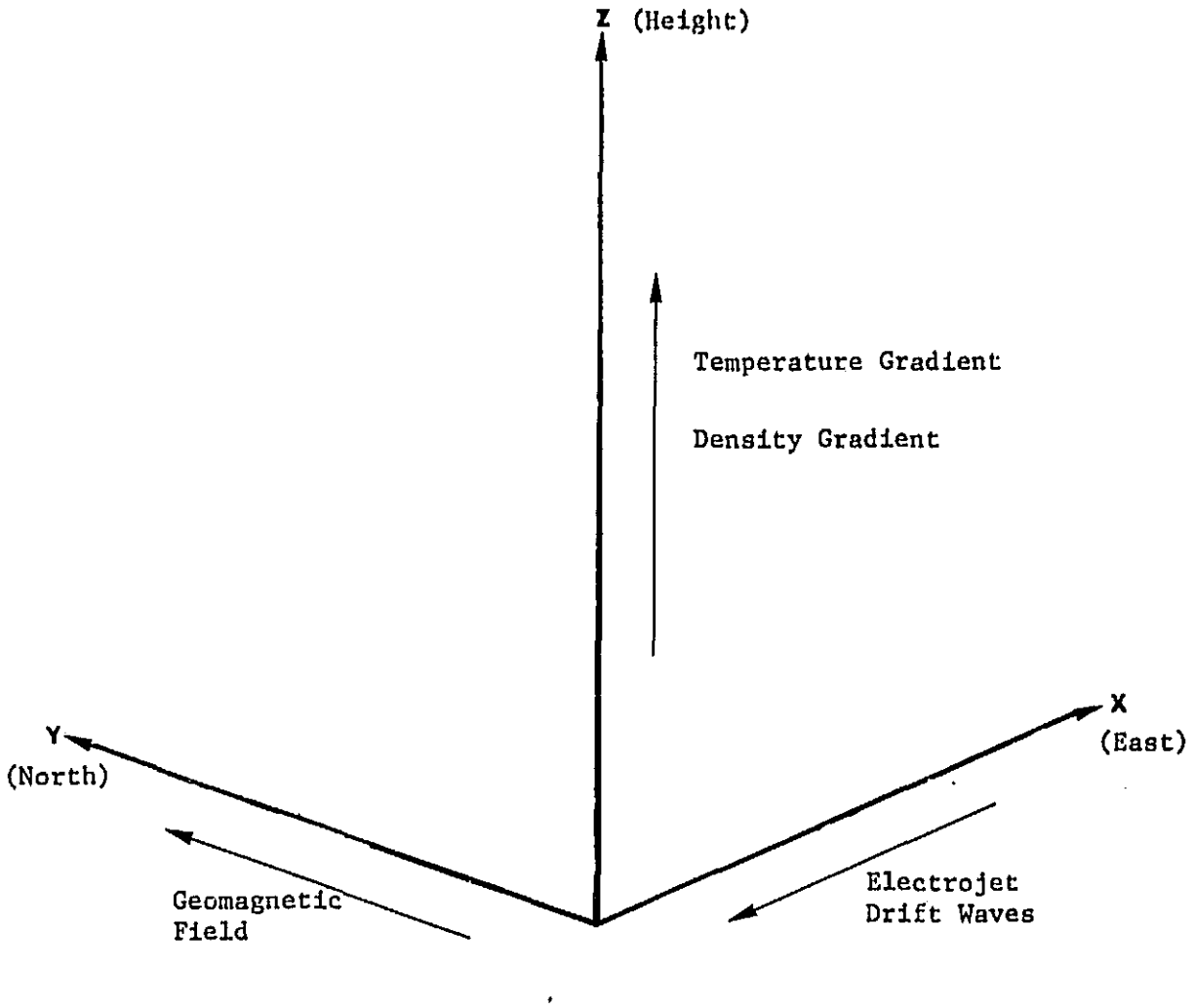
Z (Height)
Temperature Gradient
Density Gradient
Y
(North)
X
(East)
Geomagnetic
Field
Electrojet
Drift Waves

Figure III-1

TABLE III-1 CHARACTERISTICS OF ELECTROJET WITHOUT DENSITY GRADIENT

Conditions: (1) $k_{nj}^{*} \to 0, \quad k_{Tj}^{*} \neq 0$

(2) Altitude = 110 km

(3) Temperature gradients are chosen from U. S. Standard Atmosphere

Phase Velocity of Drift Waves (Westward) (m/sec)	Growth Rate of Drift Waves (Im ω/Re ω)
384	0.06
358	0.13
303	0.17

TABLE III-2 CHARACTERISTICS OF ELECTROJET WITHOUT TEMPERATURE GRADIENT

Conditions: (1) $k_{Tj}^{*} \to 0, \quad k_{nj}^{*} \neq 0$

(2) Altitude = 110 km

(3) Density gradients are chosen from U. S. Standard Atmosphere

Phase Velocity of Drift Waves (Westward) (m/sec)	Growth Rate of Drift Waves (Im ω/Re ω)
329	0.12
359	0.08
370	0.08
395	0.04

TABLE III-3 CHARACTERISTICS OF ELECTROJET WITH DENSITY AND TEMPERATURE GRADIENTS

Conditions: (1) $k^*_{nj} \neq 0$ and $k^*_{Tj} \neq 0$

(2) Altitude = 110 km

(3) Density and temperature gradients are chosen from U.S. Standard Atmosphere

Phase Velocity of Drift Waves (Westward) (m/sec)	Growth Rate of Drift Waves ($Im\omega/Re\,\omega$)
180	3.06
180	2.85
196	2.32
229	1.90
248	2.24
259	1.7
289	1.82
303	1.51
307	1.56

APPENDIX

PARTICLE VELOCITIES AND MOBILITY TENSORS IN INHOMOGENEOUS THREE-FLUID MODEL

Dynamics of particle acceleration and wave excitation are governed by the fundamental equations of three-fluid model shown in equations (1)-(5). If we assume that the inhomogeneities of temperatures and densities for three species of particles are mainly along the vertical height, we have the expressions equations (6) and (7). If we consider only the small amplitude fluctuations which are sinusoidal, fundamental equations can be rewritten as equations (8) - (12) after substituting equations (6) and (7) and linearization. To solve the equations (8) - (12) together with Maxwell's equations, let us assume that the waves are mainly propagating in north-east plane. Then, the velocity of neutral particles can be obtained in terms of the velocity of ion particles

$$\begin{bmatrix} \delta v_n^x \\ \delta v_n^y \\ \delta v_n^z \end{bmatrix} = \begin{bmatrix} \xi_n^x & \xi_n^y & \xi_n^z \\ \eta_n^x & \eta_n^y & \eta_n^z \\ \zeta_n^x & \zeta_n^y & \zeta_n^z \end{bmatrix} \begin{bmatrix} \delta v_i^x \\ \delta v_i^y \\ \delta v_i^z \end{bmatrix} \qquad \text{(A-1)}$$

where

$$\xi_n^x = i \frac{1}{D_n} \frac{\nu_{ni}}{\omega} \left[\left(1 + i \frac{\nu_{ni}}{\omega} - \frac{6 a_n^2 k_{Tn}^* k_{nn}^*}{5\omega^2} \right) \left(1 + i \frac{\nu_{ni}}{\omega} - \frac{a_n^2 k_{||}^2}{\omega^2} \right) \right.$$

$$\left. + \frac{9 a_n^4 k_{||}^2}{25 \omega^4} \left(k_{Tn}^* - k_{nn}^* \right) \left(k_{Tn}^* - \frac{2}{5} k_{nn}^* \right) \right]$$

$$\xi_n^y = i \frac{1}{D_n} \frac{\nu_{ni}}{\omega} \left[\frac{9\, a_n^4\, k_\perp\, k_\parallel}{25\omega^4} \left(k_{Tn}^* - k_{nn}^*\right) \left(k_{Tn}^* - \frac{2}{3} k_{nn}^*\right) - \frac{a_n^2\, k_\perp\, k_\parallel}{\omega^2} \left(1 + i \frac{\nu_{ni}}{\omega} - \frac{6\, a_n^2\, k_{Tn}^*\, k_{nn}^*}{5\omega^2}\right)\right]$$

$$\xi_n^z = \frac{1}{D_n} \frac{\nu_{ni}}{\omega} \frac{3\, a_n^2\, k_\perp \left(k_{Tn}^* - k_{nn}^*\right)}{5\omega^2} \left(1 + i \frac{\nu_{ni}}{\omega}\right)$$

$$\eta_n^x = i \frac{1}{D_n} \frac{\nu_{ni}}{\omega} \left[- \frac{9\, a_n^4\, k_\parallel\, k_\perp \left(k_{Tn}^* - k_{nn}^*\right)}{5\omega^4} \left(k_{Tn}^* - \frac{2}{3} k_{nn}^*\right) + \frac{a_n^2\, k_\perp\, k_\parallel}{\omega^2} \left(1 + i \frac{\nu_{ni}}{\omega} - \frac{6\, a_n^2\, k_{Tn}^*\, k_{nn}^*}{5\omega^2}\right)\right]$$

$$\eta_n^y = -i \frac{1}{D_n} \frac{\nu_{ni}}{\omega} \left[\left(1 + i \frac{\nu_{ni}}{\omega} - \frac{a_n^2\, k_\perp^2}{\omega^2}\right) \left(1 + i \frac{\nu_{ni}}{\omega} - \frac{6\, a_n^2\, k_{Tn}^*\, k_{nn}^*}{5\omega^2}\right) + \frac{9\, a_n^4\, k_\perp^2 \left(k_{Tn}^* - k_{nn}^*\right)}{5\omega^4} \left(k_{Tn}^* - \frac{2}{3} k_{nn}^*\right)\right]$$

$$\eta_n^z = \frac{1}{D_n} \frac{\nu_{ni}}{\omega} \frac{3\, a_n^2\, k_\parallel \left(k_{Tn}^* - k_{nn}^*\right)}{5\omega^2} \left(1 + i \frac{\nu_{ni}}{\omega}\right)$$

$$\zeta_n^x = \frac{1}{D_n} \frac{\nu_{ni}}{\omega} \frac{3\, a_n^2\, k_\perp}{5\omega^2} \left(k_{Tn}^* - \frac{2}{3} k_{nn}^*\right) \left(1 + i \frac{\nu_{ni}}{\omega}\right)$$

$$\zeta_n^y = - \frac{1}{D_n} \frac{\nu_{ni}}{\omega} \frac{3\, a_n^2\, k_\parallel}{5\omega^2} \left(k_{Tn}^* - \frac{2}{3} k_{nn}^*\right) \left(1 + i \frac{\nu_{ni}}{\omega}\right)$$

$$\zeta_n^z = i \frac{1}{D_n} \frac{\nu_{ni}}{\omega} \left(1 + i \frac{\nu_{ni}}{\omega}\right) \left(1 + i \frac{\nu_{ni}}{\omega} - \frac{a_n^2 k^2}{\omega^2}\right)$$

and

$$D_n = \left(1 + i \frac{\nu_{ni}}{\omega} - \frac{6 a_n^2 k_{Tn}^* k_{nn}^*}{5\omega^2}\right) \left(1 + 2i \frac{\nu_{ni}}{\omega} - \frac{a_n^2 k^2}{\omega^2} - i \frac{a_n^2 k^2 \nu_{ni}}{\omega^3} - \frac{\nu_{ni}}{\omega^2}\right) + \frac{18 a_n^6 k_\perp^2 k_{||}^2}{25\omega^6} \left(k_{Tn}^* - k_{nn}^*\right) \left(k_{Tn}^* - \frac{2}{3} k_{nn}^*\right)$$

$$+ \frac{9 a_n^4}{25\omega^4} \left(k_{Tn}^* - k_{nn}^*\right) \left(k_{Tn}^* - \frac{2}{3} k_{nn}^*\right) \left[k^2 \left(1 + i \frac{\nu_{ni}}{\omega}\right) - \frac{2 a_n^2 k_{||}^2 k_\perp^2}{\omega^2}\right]$$

Here, subscripts $\perp$ and $||$ denote the components perpendicular and parallel to the geomagnetic field, respectively. In the present model, subscripts $\perp$ and $||$ particularly imply the components along east and north directions, respectively.

Velocity of ion particles can be solved in terms of mobility tensor, i.e.,

$$\begin{bmatrix} \delta v_i^x \\ \delta v_i^y \\ \delta v_i^z \end{bmatrix} = \frac{C}{\langle B \rangle} \begin{bmatrix} \xi_i^x & \xi_i^y & \xi_i^z \\ \eta_i^x & \eta_i^y & \eta_i^z \\ \zeta_i^x & \zeta_i^y & \zeta_i^z \end{bmatrix} \begin{bmatrix} \delta E_x \\ \delta E_y \\ \delta E_z \end{bmatrix} \qquad \text{(A-2)}$$

where

$$\xi_i^x = i\,\frac{1}{D_i}\left\{\left(\frac{\omega}{\Omega_i} + i\,\frac{\nu_{in}}{\Omega_i}\,(1-\eta_n^y) - \frac{6\,a_i^2\,k_{ni}^*\,k_{Ti}^*}{5\,\Omega_i\omega}\right)\left[\frac{\omega}{\Omega_i}\right.\right.$$

$$\left. + i\,\frac{\nu_{in}}{\Omega_i}\,(1-\zeta_n^y) - \frac{a_i^2\,k_{||}^2}{\Omega_i\omega}\right] + \left[\frac{3a_i^2\,k_{||}}{5\,\Omega_i\omega}\left(\frac{2}{3}\,k_{ni}^* - k_{Ti}^*\right)\right.$$

$$\left.\left. + \frac{\nu_{in}}{\Omega_i}\,\eta_n^z\right]\left[\frac{3\,a_i^2\,k_{||}}{5\Omega_i\omega}\,(k_{ni}^* - k_{Ti}^*) + i\,\frac{\nu_{in}}{\Omega_i}\,\zeta_n^y\right]\right\}$$

$$\xi_i^y = i\,\frac{1}{D_i}\left\{\left[1 + \frac{3\,a_i^2\,k_{\perp}}{\Omega_i\omega}\,(k_{ni}^* - k_{Ti}^*) + \frac{\nu_{in}}{\Omega_i}\,\xi_n^y\right]\cdot\right.$$

$$\cdot\left[\frac{3\,a_i^2\,k_{||}}{5\,\Omega_i\omega}\,\left(\frac{2}{3}\,k_{ni}^* - k_{Ti}^*\right) + \frac{\nu_{in}}{\Omega_i}\,\eta_n^y\right] - \left(\frac{a_i^2\,k_{\perp}\,k_{||}}{\Omega_i\omega}\right.$$

$$\left.\left. + i\,\frac{\nu_{in}}{\Omega_i}\,\xi_n^z\right)\left[\frac{\omega}{\Omega_i} + i\,\frac{\nu_{in}}{\Omega_i}\,(1-\eta_n^y) - \frac{6\,a_i^2\,k_{ni}^*\,k_{Ti}^*}{5\Omega_i\omega}\right]\right\}$$

$$\xi_i^z = -\,\frac{1}{D_i}\left\{\left(\frac{a_i^2\,k_{\perp}\,k_{||}}{\Omega_i\omega} + i\,\frac{\nu_{in}}{\Omega_i}\,\xi_n^z\right)\left[\frac{3\,a_i^2\,k_{||}}{5\Omega_i\omega}\,(k_{ni}^* - k_{Ti}^*)\right.\right.$$

$$\left. + \frac{\nu_{in}}{\Omega_i}\,\zeta_n^y\right] + \left[1 + \frac{3\,a_i^2\,k_{\perp}}{\Omega_i\omega}\,(k_{ni}^* - k_{Ti}^*) + \frac{\nu_{in}}{\Omega_i}\,\xi_n^y\right]\cdot$$

$$\left.\cdot\left[\frac{\omega}{\Omega_i} + i\,\frac{\nu_{in}}{\Omega_i}\,(1-\zeta_n^z) - \frac{a_i^2\,k_{||}^2}{\Omega_i\omega}\right]\right\}$$

$$\eta_i^x = i\,\frac{1}{D_i}\left\{\left[1 - \frac{3\,a_i^2\,k_{\perp}}{5\Omega_i\omega}\,\left(\frac{2}{3}\,k_{ni}^* - k_{Ti}^*\right) - \frac{\nu_{in}}{\Omega_i}\,\eta_n^x\right]\left[\frac{3\,a_i^2\,k_{||}}{5\Omega_i\omega}\cdot\right.\right.$$

$$\cdot (k_{ni}^* - k_{Ti}^*) + \frac{\nu_{in}}{\Omega_i} \zeta_n^y \Big] + \Big[\frac{\omega}{\Omega_i} + i \frac{\nu_{in}}{\Omega_i} (1 - \eta_n^y) - \frac{6 a_i^2 k_{ni}^* k_{Ti}^*}{5\Omega_i\omega}\Big] \Big(\frac{a_i^2 k_\perp k_\parallel}{\Omega_i\omega} + i \frac{\nu_{in}}{\Omega_i} \zeta_n^x\Big)\Big\}$$

$$\eta_i^y = i \frac{1}{D_i} \Big\{-\Big[\frac{\omega}{\Omega_i} + i \frac{\nu_{in}}{\Omega_i} (1 - \xi_n^x) - \frac{a_i^2 k_\perp^2}{\Omega_i\omega}\Big]\Big[\frac{\omega}{\Omega_i} + i \frac{\nu_{in}}{\Omega_i} (1 - \eta_n^y) - \frac{6 a_i^2 k_{ni}^* k_{Ti}^*}{5\Omega_i\omega}\Big] + \Big[1 + \frac{3 a_i^2 k_\perp}{\Omega_i\omega} (k_{ni}^* - k_{Ti}^*) + \frac{\nu_{in}}{\Omega_i} \xi_n^y\Big]\Big[1 - \frac{3 a_i^2 k_\perp}{5\Omega_i\omega} (\frac{2}{3} k_{ni}^* - k_{Ti}^*) - \frac{\nu_{in}}{\Omega_i} \eta_n^x\Big]\Big\}$$

$$\eta_i^z = - \frac{1}{D_i} \Big\{\Big(\frac{a_i^2 k_\perp k_\parallel}{\Omega_i\omega} + i \frac{\nu_{in}}{\Omega_i} \zeta_n^x\Big)\Big[1 + \frac{3a_i^2 k_\perp}{\Omega_i\omega} (k_{ni}^* - k_{Ti}^*) + \frac{\nu_{in}}{\Omega_i} \xi_n^y\Big] + \Big[\frac{\omega}{\Omega_i} + i \frac{\nu_{in}}{\Omega_i} (1 - \xi_n^x) - \frac{a_i^2 k_\perp^2}{\Omega_i\omega}\Big]\Big[\frac{3 a_i^2 k_\parallel}{5\Omega_i\omega} \cdot (k_{ni}^* - k_{Ti}^*) + \frac{\nu_{in}}{\Omega_i} \zeta_n^y\Big]\Big\}$$

$$\zeta_i^x = \frac{1}{D_i} \Big\{- \Big(\frac{a_i^2 k_\perp k_\parallel}{\Omega_i\omega} + i \frac{\nu_{in}}{\Omega_i} \zeta_n^x\Big)\Big[\frac{3 a_i^2 k_\parallel}{5\Omega_i\omega} (\frac{2}{3} k_{ni}^* - k_{Ti}^*) + \frac{\nu_{in}}{\Omega_i} \eta_n^z\Big] + \Big[1 - \frac{3 a_i^2 k_\perp}{5\Omega_i\omega} (\frac{2}{3} k_{ni}^* - k_{Ti}^*) - \frac{\nu_{in}}{\Omega_i} \eta_n^x\Big] \cdot \Big[\frac{\omega}{\Omega_i} + i \frac{\nu_{in}}{\Omega_i} (1 - \zeta_n^z) - \frac{a_i^2 k_\parallel^2}{\Omega_i\omega}\Big]\Big\}$$

$$\zeta_i^y = \frac{1}{D_i} \left\{ - \left(\frac{a_i^2 k_\perp k_\parallel}{\Omega_i \omega} + i \frac{\nu_{in}}{\Omega_i} \xi_n^z \right) \left[1 - \frac{3 a_i^2 k_\perp}{5 \Omega_i \omega} \left(\frac{2}{3} k_{ni}^* - k_{Ti}^* \right) - \frac{\nu_{in}}{\Omega_i} \eta_n^x \right] + \left[\frac{\omega}{\Omega_i} + i \frac{\nu_{in}}{\Omega_i} (1 - \xi_n^x) - \frac{a_i^2 k_\perp^2}{\Omega_i \omega} \right] \cdot \right.$$

$$\left. \cdot \left[\frac{3 a_i^2 k_\parallel}{5 \Omega_i \omega} \left(\frac{2}{3} k_{ni}^* - k_{Ti}^* \right) + \frac{\nu_{in}}{\Omega_i} \eta_n^z \right] \right\}$$

$$\zeta_i^z = i \frac{1}{D_i} \left\{ \left[\frac{\omega}{\Omega_i} + i \frac{\nu_{in}}{\Omega_i} (1 - \xi_n^x) - \frac{a_i^2 k_\perp^2}{\Omega_i \omega} \right] \left[\frac{\omega}{\Omega_i} + i \frac{\nu_{in}}{\Omega_i} (1 - \zeta_n^z) - \frac{a_i^2 k_\parallel^2}{\Omega_i \omega} \right] - \left(\frac{a_i^2 k_\perp k_\parallel}{\Omega_i \omega} + i \frac{\nu_{in}}{\Omega_i} \zeta_n^x \right) \cdot \right.$$

$$\left. \cdot \left(\frac{a_i^2 k_\perp k_\parallel}{\Omega_i \omega} + i \frac{\nu_{in}}{\Omega_i} \right) \xi_n^z \right\}$$

and

$$D_i = \left[\frac{\omega}{\Omega_i} + i \frac{\nu_{in}}{\Omega_i} (1 - \xi_n^x) - \frac{a_i^2 k_\perp^2}{\Omega_i \omega} \right] \left[\frac{\omega}{\Omega_i} + i \frac{\nu_{in}}{\Omega_i} (1 - \eta_n^y) - \frac{6 a_i^2 k_{ni}^* k_{Ti}^*}{5 \Omega_i \omega} \right] \left[\frac{\omega}{\Omega_i} + i \frac{\nu_{in}}{\Omega_i} (1 - \zeta_n^z) - \frac{a_i^2 k_\parallel^2}{\Omega_i \omega} \right] - \left(\frac{a_i k_\perp k_\parallel}{\Omega_i \omega} \right.$$

$$\left. + i \frac{\nu_{in}}{\Omega_i} \xi_n^z \right) \left[\frac{3 a_i^2 k_\parallel}{5 \Omega_i \omega} (k_{ni}^* - k_{Ti}^*) + \frac{\nu_{in}}{\Omega_i} \zeta_n^y \right] \left[1 - \frac{3 a_i^2 k_\perp}{5 \Omega_i \omega} \cdot \right.$$

$$\left. \cdot \left(\frac{2}{3} k_{ni}^* - k_{Ti}^* \right) - \frac{\nu_{in}}{\Omega_i} \eta_n^x \right] + \left(\frac{a_i^2 k_\perp k_\parallel}{\Omega_i \omega} + i \frac{\nu_{in}}{\Omega_i} \zeta_n^x \right) \left[1 + \right.$$

$$\left. + \frac{3 a_i^2 k_\perp}{\Omega_i \omega} (k_{ni}^* - k_{Ti}^*) + \frac{\nu_{in}}{\Omega_i} \xi_n^y \right] \left[\frac{3 a_i^2 k_\parallel}{5 \Omega_i \omega} \left(\frac{2}{3} k_{ni}^* - k_{Ti}^* \right) \right.$$

$$\left. + \frac{\nu_{in}}{\Omega_i} \eta_n^z \right] - \left(\frac{a_i^2 k_\perp k_\parallel}{\Omega_i \omega} + i \frac{\nu_{in}}{\Omega_i} \xi_n^z \right) \left(\frac{a_i^2 k_\perp k_\parallel}{\Omega_i \omega} + i \frac{\nu_{in}}{\Omega_i} \zeta_n^x \right)$$

$$\cdot \left[\frac{\omega}{\Omega_i} + i\frac{\nu_{in}}{\Omega_i}(1 - \eta_n^y) - \frac{6\,a_i^2\,k_{ni}^*\,k_{Ti}^*}{5\Omega_i\omega}\right] - \left[1 + \right.$$

$$\left. + \frac{3\,a_i^2\,k_\perp}{\Omega_i\omega}(k_{ni}^* - k_{Ti}^*) + \frac{\nu_{in}}{\Omega_i}\xi_n^y\right]\left[1 - \frac{3\,a_i^2\,k_\perp}{5\Omega_i\omega}\left(\frac{2}{3}k_{ni}^* - k_{Ti}^*\right)\right.$$

$$\left. - \frac{\nu_{in}}{\Omega_i}\eta_n^x\right]\left[\frac{\omega}{\Omega_i} + i\frac{\nu_{in}}{\Omega_i}(1 - \zeta_n^z) - \frac{a_i^2\,k_\parallel^2}{\Omega_i\omega}\right] + \left[\frac{3\,a_i^2\,k_\perp k_\parallel}{5\Omega_i\omega}\right.\cdot$$

$$\cdot\left(\frac{2}{3}k_{ni}^* - k_{Ti}^*\right) + \frac{\nu_{in}}{\Omega_i}\eta_n^z\left]\left[\frac{3\,a_i^2\,k_\parallel}{5\Omega_i\omega}(k_{ni}^* - k_{Ti}^*) + \frac{\nu_{in}}{\Omega_i}\zeta_n^y\right]\right.\cdot$$

$$\cdot\left[\frac{\omega}{\Omega_i} + i\frac{\nu_{in}}{\Omega_i}(1 - \xi_n^x) - \frac{a_i^2\,k_\perp^2}{\Omega_i\omega}\right]$$

Finally, velocity of electron particles also can be solved in terms of mobility tensor, i.e.,

$$\begin{bmatrix}\delta v_e^x\\ \delta v_e^y\\ \delta v_e^z\end{bmatrix} = \frac{C}{\langle B\rangle}\begin{bmatrix}\xi_e^x & \xi_e^y & \xi_e^z\\ \eta_e^x & \eta_e^y & \eta_e^z\\ \zeta_e^x & \zeta_e^y & \zeta_e^z\end{bmatrix}\begin{bmatrix}\delta E_x\\ \delta E_y\\ \delta E_z\end{bmatrix} \qquad \text{(A-3)}$$

where

$$\xi_e^x = i\frac{1}{D_e}\left\{\left[\frac{\nu_{en}}{\Omega_e}(\xi_n^x\,\xi_i^x + \xi_n^y\,\eta_i^x + \xi_n^z\,\zeta_i^x) + \frac{\nu_{ei}}{\Omega_e}\xi_i^x - 1\right]\cdot\right.$$

$$\cdot\left[\left(i\frac{\nu_{en}}{\Omega_e} + i\frac{\nu_{ei}}{\Omega_e} - \frac{6\,a_e^2\,k_{Te}^*\,k_{ne}^*}{5\Omega_e\omega}\right)\left(i\frac{\nu_{en}}{\Omega_e} + i\frac{\nu_{ei}}{\Omega_e} - \frac{a_e^2\,k_\parallel^2}{\Omega_e\omega}\right)\right.$$

$$\left. + \frac{9\,a_e^4\,k_\parallel^2}{25\Omega_e^2\omega^2}(k_{ne}^* - k_{Te}^*)\left(\frac{2}{3}k_{ne}^* - k_{Te}^*\right)\right] + \left[\frac{\nu_{en}}{\Omega_e}\left(\eta_n^x\,\xi_i^x\right.\right.$$

$$+ \eta_n^y \eta_i^x + \eta_n^z \zeta_i^x) + \frac{\nu_{ei}}{\Omega_e} \eta_i^x \Big] \Big[i \frac{3 a_e^4 k_{||}^2 k_\perp}{5\Omega_e^2\omega^2} (k_{ne}^* - k_{Te}^*)$$

$$- i \left(i \frac{\nu_{ei}}{\Omega_e} + i \frac{\nu_{ei}}{\Omega_e} - \frac{a_e^2 k_{||}^2}{\Omega_e \omega} \right) \left[1 - \frac{3 a_e^2 k_\perp}{5\Omega_e\omega} (k_{ne}^* - k_{Te}^*) \right] \Big]$$

$$+ \left[\frac{\nu_{en}}{\Omega_e} (\zeta_n^x \xi_i^x + \zeta_n^y \eta_i^x + \zeta_n^z \zeta_i^x) + \frac{\nu_{ei}}{\Omega_e} \zeta_i^x \right] \left[\frac{3 a_e^2 k_{||}}{5\Omega_e\omega} \cdot \right.$$

$$\cdot \left(\frac{2}{3} k_{ne}^* - k_{Te}^*\right) \left[1 - \frac{3 a_e^2 k_\perp}{5\Omega_e\omega} (k_{ne}^* - k_{Te}^*) \right] + \frac{a_e^2 k_\perp k_{||}}{\Omega_e\omega} \cdot$$

$$\left. \cdot \left(i \frac{\nu_{en}}{\Omega_e} + i \frac{\nu_{ei}}{\Omega_e} - \frac{6 a_e^2 k_{Te}^* k_{ne}^*}{5\Omega_e\omega} \right) \right] \Big\}$$

$$\xi_e^y = -i \frac{1}{D_e} \Big\{ \Big[\frac{\nu_{en}}{\Omega_e} (\xi_n^x \xi_i^z + \xi_n^y \eta_i^z + \xi_n^z \zeta_i^z) + \frac{\nu_{ei}}{\Omega_e} \xi_i^z \Big] \Big[\Big(i \frac{\nu_{en}}{\Omega_e} + \frac{\nu_{ei}}{\Omega_e}$$

$$- \frac{6 a_e^2 k_{Te}^* k_{ne}^*}{5\Omega_e\omega} \Big) \left(i \frac{\nu_{en}}{\Omega_e} + i \frac{\nu_{ei}}{\Omega_e} - \frac{a_e^2 k_{||}^2}{\Omega_e\omega} \right) + \frac{9 a_e^4 k_{||}^2}{25\Omega_e^2\omega^2} (k_{ne}^* - k_{Te}^*) \cdot$$

$$\cdot \left(\frac{2}{3} k_{ne}^* - k_{Te}^*\right) \Big] + \Big[\frac{\nu_{en}}{\Omega_e} (\eta_n^x \xi_i^z + \eta_n^y \eta_i^z + \eta_n^z \zeta_i^z) + \frac{\nu_{ei}}{\Omega_e} \eta_i^z \Big] \cdot$$

$$\cdot \Big[i \frac{3 a_e^4 k_{||}^2 k_\perp}{5\Omega_e^2\omega^2} (k_{ne}^* - k_{Te}^*) - i \Big(\frac{\nu_{en}}{\Omega_e} + i \frac{\nu_{ei}}{\Omega_e} - \frac{a_e^2 k_{||}^2}{\Omega_e \omega} \Big) \Big(1$$

$$- \frac{3 a_e^2 k_\perp}{5\Omega_e\omega} (k_{ne}^* - k_{Te}^*) \Big) \Big] + \Big[\frac{\nu_{en}}{\Omega_e} (\zeta_n^x \xi_i^z + \zeta_n^y \eta_i^z + \zeta_n^z \zeta_i^z)$$

$$+ \frac{\nu_{ei}}{\Omega_e} \zeta_i^z - 1 \Big] \Big[\frac{3 a_e^2 k_{||}}{5\Omega_e\omega} \left(\frac{2}{3} k_{ne}^* - k_{Te}^*\right) \left(1 - \frac{3 a_e^2 k_\perp}{5\Omega_e\omega} (k_{ne}^* - k_{Te}^*) \right)$$

$$+ \frac{a_e^2 k_\perp k_{||}}{\Omega_e\omega} \left(i \frac{\nu_{en}}{\Omega_e} + i \frac{\nu_{ei}}{\Omega_e} - \frac{6 a_e^2 k_{Te}^* k_{ne}^*}{5\Omega_e\omega} \right) \Big] \Big\}$$

$$\xi_e^z = i\frac{1}{D_e}\left\{\left[\frac{\nu_{en}}{\Omega_e}(\xi_n^x\xi_i^y + \xi_n^y\eta_i^y + \xi_n^z\zeta_i^y) + \frac{\nu_{ei}}{\Omega_e}\xi_i^y\right]\left[\left(i\frac{\nu_{en}}{\Omega_e}\right.\right.\right.$$

$$+ i\frac{\nu_{ei}}{\Omega_e} - \frac{6\,a_e^2\,k_{Te}^*\,k_{ne}^*}{5\Omega_e\omega}\Big)\left(i\frac{\nu_{en}}{\Omega_e} + i\frac{\nu_{ei}}{\Omega_e} - \frac{a_e^2\,k_{\|}^2}{\Omega_e\,\omega}\right) + \frac{9a_e^4k_{\|}^2}{25\Omega_e^2\omega^2}\cdot$$

$$\cdot(k_{ne}^* - k_{Te}^*)\left(\frac{2}{3}k_{ne}^* - k_{Te}^*\right)\Big] + \Big[\frac{\nu_{en}}{\Omega_e}(\eta_n^x\xi_i^y + \eta_n^y\eta_i^y$$

$$+ \eta_n^z\zeta_i^y) + \frac{\nu_{ei}}{\Omega_e}\eta_i^y - 1\Big]\Big[i\frac{3\,a_e^4\,k_{\|}^2k_{\perp}}{5\Omega_e^2\omega^2}(k_{ne}^* - k_{Te}^*)$$

$$- i\left(i\frac{\nu_{en}}{\Omega_e} + i\frac{\nu_{ei}}{\Omega_e} - \frac{a_e^2\,k_{\|}^2}{\Omega_e\,\omega}\right)\left(1 - \frac{3a_e^2\,k_{\perp}}{5\Omega_e\omega}(k_{ne}^* - k_{Te}^*)\right)\Big]$$

$$+ \Big[\frac{\nu_{en}}{\Omega_e}(\zeta_n^x\xi_i^y + \zeta_n^y\eta_i^y + \zeta_n^z\zeta_i^y) + \frac{\nu_{ei}}{\Omega_e}\zeta_i^y\Big]\Big[\frac{3\,a_e^2\,k_{\|}}{5\Omega_e\omega}\cdot$$

$$\cdot\left(\frac{2}{3}k_{ne}^* - k_{Te}^*\right)\left(1 - \frac{3\,a_e^2\,k_{\perp}}{5\Omega_e\omega}(k_{ne}^* - k_{Te}^*)\right)\frac{a_e^2\,k_{\perp}k_{\|}}{\Omega_e\omega}\left(i\frac{\nu_{en}}{\Omega_e} + \frac{\nu_{ei}}{\Omega_e}\right.$$

$$\left.\left.\left.\left. - \frac{6\,a_e^2\,k_{Te}^*\,k_{ne}^*}{5\Omega_e\omega}\right)\Big]\right\}\right.$$

$$\eta_e^x = i\frac{1}{D_e}\left\{\left[\frac{\nu_{en}}{\Omega_e}(\zeta_n^x\xi_i^x + \zeta_n^y\eta_i^x \pm \zeta_n^z\zeta_i^x) + \frac{\nu_{ei}}{\Omega_e}\zeta_i^x\right]\left[i\frac{\nu_{en}}{\Omega_e}\right.\right.$$

$$+ i\frac{\nu_{ei}}{\Omega_e} - \frac{a_e^2\,k_{\perp}^2}{\Omega_e\omega}\Big)\left(i\frac{\nu_{en}}{\Omega_e} + i\frac{\nu_{ei}}{\Omega_e} - \frac{6\,a_e^2\,k_{Te}^*\,k_{ne}^*}{5\Omega_e\omega}\right) - \left(1 - \frac{3a_e^2\,k_{\perp}}{5\Omega_e\omega}\cdot\right.$$

$$\left.\cdot(k_{ne}^* - k_{Te}^*)\right)\left(1 + \frac{3a_e^2\,k_{\perp}}{5\Omega_e\omega}\left(\frac{2}{3}k_{ne}^* - k_{Te}^*\right)\right)\Big] + \Big[\frac{\nu_{en}}{\Omega_e}(\xi_n^x\xi_i^x$$

$$+ \xi_n^y\eta_i^x + \xi_n^z\zeta_i^x) + \frac{\nu_{ei}}{\Omega_e}\xi_i^x - 1\Big]\Big[-\frac{3\,a_e^2\,k_{\|}}{5\Omega_e\omega}(k_{ne}^* - k_{Te}^*)\cdot$$

$$\cdot \left(1 + \frac{3\, a_e^2\, k_\perp}{5\Omega_e\omega}\ \left(\frac{2}{3}\, k_{ne}^* - k_{Te}^*\right)\right) + \frac{a_e^2\, k_\perp k_\parallel}{\Omega_e\omega}\left(i\,\frac{\nu_{en}}{\Omega_e} + i\,\frac{\nu_{ei}}{\Omega_e}\right.$$

$$\left. - \frac{6\, a_e^2\, k_{Te}^*\, k_{ne}^*}{5\Omega_e\omega}\right)\Bigg] + \left[\frac{\nu_{en}}{\Omega_e}\left(\eta_n^x\, \xi_i^x + \eta_n^y\, \eta_i^x + \eta_n^z\, \zeta_i^x\right) + \frac{\nu_{ei}}{\Omega_e}\,\eta_i^x\right] \cdot$$

$$\cdot \left[-i\,\frac{a_e^2\, k_\perp k_\parallel}{\Omega_e\omega}\left(1 - \frac{3a_e^2\, k_\perp}{5\Omega_e\omega}\ (k_{ne}^* - k_{Te}^*)\right) + i\,\frac{3a_e^2 k_\parallel}{5\Omega_e\omega}\ (k_{ne}^* - k_{Te}^*) \cdot\right.$$

$$\left.\cdot\ i\,\frac{\nu_{en}}{\Omega_e} + i\,\frac{\nu_{ei}}{\Omega_e} - \frac{a_e^2\, k_\perp^2}{\Omega_e\omega}\right)\Bigg]\Bigg\}$$

$$\eta_e^y = -i\,\frac{1}{D_e}\left\{\left[\frac{\nu_{en}}{\Omega_e}\left(\zeta_n^x\, \xi_i^z + \zeta_n^y\, \eta_i^z + \zeta_n^z\, \zeta_i^z\right) + \frac{\nu_{ei}}{\Omega_e}\,\zeta_i^z - 1\right]\left[\left(i\,\frac{\nu_{en}}{\Omega_e}\right.\right.\right.$$

$$\left. + i\,\frac{\nu_{ei}}{\Omega_e} - \frac{a_e^2\, k_\perp^2}{\Omega_e\omega}\right)\left(i\,\frac{\nu_{en}}{\Omega_e} + i\,\frac{\nu_{ei}}{\Omega_e} - \frac{6\, a_e^2\, k_{Te}^*\, k_{ne}^*}{5\Omega_e\omega}\right) - \left(1 - \frac{3\, a_e^2\, k_\perp}{5\Omega_e\omega}\right. \cdot$$

$$\left.\cdot\ (k_{ne}^* - k_{Te}^*)\right)\left(1 + \frac{3\, a_e^2\, k_\perp}{5\Omega_e\omega}\ \left(\frac{2}{3}\, k_{ne}^* - k_{Te}^*\right)\right)\Bigg] + \left[\frac{\nu_{en}}{\Omega_e}\left(\xi_n^x\, \xi_i^z\right.\right.$$

$$\left.\left. + \xi_n^y\, \eta_i^z + \xi_n^z\, \zeta_i^z\right) + \frac{\nu_{ei}}{\Omega_e}\,\xi_i^z\right]\left[-\frac{3\, a_e^2\, k_\parallel}{5\Omega_e\omega}\ (k_{ne}^* - k_{Te}^*)\ \left(1 + \frac{3\, a_e^2 k_\perp}{5\Omega_e\omega}\right.\right. \cdot$$

$$\left.\left.\cdot\ (k_{ne}^* - k_{Te}^*)\ \left(1 + \frac{3\, a_e^2\, k_\perp}{5\Omega_e\omega}\ \left(\frac{2}{3}\, k_{ne}^* - k_{Te}^*\right)\right)\ \frac{a_e^2\, k_\perp\, k_\parallel}{\Omega_e\omega}\cdot\left(i\,\frac{\nu_{en}}{\Omega_e}\right.\right.\right.$$

$$\left.\left.\left. + i\,\frac{\nu_{ei}}{\Omega_e} - \frac{6\, a_e^2\, k_{Te}^*\, k_{ne}^*}{5\Omega_e\omega}\right)\right] + \left[\frac{\nu_{en}}{\Omega_e}\left(\eta_n^x\, \xi_i^z + \eta_n^y\, \eta_i^z + \eta_n^z\, \zeta_i^z\right)\right.$$

$$\left.\left. + \frac{\nu_{ei}}{\Omega_e}\ \eta_i^z\right]\left[-i\,\frac{a_e^2\, k_\perp k_\parallel}{\Omega_e\omega}\ \left(1 - \frac{3\, a_e^2\, k_\perp}{5\Omega_e\omega}\ (k_{ne}^* - k_{Te}^*)\right) + i\,\frac{3a_e^2 k_\parallel}{5\Omega_e\omega}\ \cdot\right.\right.$$

$$\cdot (k^*_{ne} - k^*_{Te}) \left(i \frac{\nu_{en}}{\Omega_e} + i \frac{\nu_{ei}}{\Omega_e} - \frac{a_e^2 k_\perp^2}{\Omega_e \omega}\right)\Bigg]\Bigg\}$$

$$\eta_e^z = i \frac{1}{D_e} \Bigg\{\Bigg[\frac{\nu_{en}}{\Omega_e} (\zeta_n^x \xi_i^y + \zeta_n^y \eta_i^y + \zeta_n^z \zeta_i^y) + \frac{\nu_{ei}}{\Omega_e} \zeta_i^y\Bigg] \Bigg[\Bigg(i \frac{\nu_{en}}{\Omega_e}$$

$$+ i \frac{\nu_{ei}}{\Omega_e} - \frac{a_e^2 k_\perp^2}{\Omega_e \omega}\Bigg)\Bigg(i \frac{\nu_{en}}{\Omega_e} + i \frac{\nu_{ei}}{\Omega_e} - \frac{6 a_e^2 k^*_{Te} k^*_{ne}}{5\Omega_e \omega}\Bigg) - \Bigg(1 - \frac{3 a_e^2 k_\perp}{5\Omega_e \omega} \cdot$$

$$\cdot (k^*_{ne} - k^*_{Te})\Bigg) \Bigg(1 + \frac{3 a_e^2 k_\perp}{5\Omega_e \omega} \left(\frac{2}{3} k^*_{ne} - k^*_{Te}\right)\Bigg)\Bigg] + \Bigg[\frac{\nu_{en}}{\Omega_e} (\xi_n^x \xi_i^y$$

$$+ \xi_n^y \eta_i^y + \xi_n^z \zeta_i^y) + \frac{\nu_{ei}}{\Omega_e} \xi_i^y\Bigg] \Bigg[- \frac{3 a_e^2 k_{||}}{5\Omega_e \omega} (k^*_{ne} - k^*_{Te}) \Bigg(1 +$$

$$+ \frac{3 a_e^2 k_\perp}{5\Omega_e \omega} \left(\frac{2}{3} k^*_{ne} - k^*_{Te}\right)\Bigg) + \frac{a_e^2 k_\perp k_{||}}{\Omega_e \omega} \Bigg(i \frac{\nu_{en}}{\Omega_e} + i \frac{\nu_{ei}}{\Omega_e} - \frac{6 a_e^2 k^*_{Te} k^*_{ne}}{5\Omega_e \omega}\Bigg)\Bigg]$$

$$+ \Bigg[\frac{\nu_{en}}{\Omega_e} (\eta_n^x \xi_i^y + \eta_n^y \eta_i^y + \eta_n^z \zeta_i^y) + \frac{\nu_{ei}}{\Omega_e} \eta_i^y - 1\Bigg] \Bigg[-i \frac{a_e^2 k_\perp k_{||}}{\Omega_e \omega} \cdot$$

$$\cdot \Bigg(1 - \frac{3 a_e^2 k_\perp}{5\Omega_e \omega} (k^*_{ne} - k^*_{Te})\Bigg) + i \frac{3 a_e^2 k_{||}}{5\Omega_e \omega} (k^*_{ne} - k^*_{Te}) \Bigg(i \frac{\nu_{en}}{\Omega_e}$$

$$+ i \frac{\nu_{ei}}{\Omega_e} - \frac{a_e^2 k_\perp^2}{\Omega_e \omega}\Bigg)\Bigg]\Bigg\} \quad .$$

$$\zeta_e^x = i \frac{1}{D_e} \Bigg\{\Bigg[\frac{\nu_{en}}{\Omega_e} (\eta_n^x \xi_i^x + \eta_n^y \eta_i^x + \eta_n^z \zeta_i^x) + \frac{\nu_{ei}}{\Omega_e} \eta_i^x\Bigg] \Bigg[\Bigg(i \frac{\nu_{en}}{\Omega_e} + i \frac{\nu_{ei}}{\Omega_e}$$

$$- \frac{a_e^2 k_\perp^2}{\Omega_e \omega}\Bigg)\Bigg(i \frac{\nu_{en}}{\Omega_e} + i \frac{\nu_{ei}}{\Omega_e} - \frac{a_e^2 k_{||}^2}{\Omega_e \omega}\Bigg) - \frac{a_e^4 k_\perp^2 k_{||}^2}{\Omega_e^2 \omega^2}\Bigg] + \Bigg[\frac{\nu_{en}}{\Omega_e} (\zeta_n^x \xi_i^x$$

$$+ \zeta_n^y \eta_i^x + \zeta_n^z \zeta_i^x) + \frac{\nu_{ei}}{\Omega_e} \zeta_i^x \Big] \Big[i \frac{a_e^2 k_\perp k_\parallel}{\Omega_e \omega} \Big(1 + \frac{3 a_e^2 k_\perp}{5\Omega_e \omega} \big(\frac{2}{3} k_{ne}^* - k_{Te}^* \big) \Big) + i \frac{3 a_e^2 k_\parallel}{5\Omega_e \omega} \big(\frac{2}{3} k_{ne}^* - k_{Te}^* \big) \Big(i \frac{\nu_{en}}{\Omega_e} + i \frac{\nu_{ei}}{\Omega_e} - \frac{a_e^2 k_\perp^2}{\Omega_e \omega} \Big) \Big]$$

$$+ \Big[\frac{\nu_{en}}{\Omega_e} (\xi_n^x \xi_i^x + \xi_n^y \eta_i^x + \xi_n^z \zeta_i^x) + \frac{\nu_{ei}}{\Omega_e} \xi_i^x - 1 \Big] \cdot$$

$$\cdot \Big[i \frac{3 a_e^4 k_\parallel^2 k_\perp}{5\Omega_e^2 \omega^2} \big(\frac{2}{3} k_{ne}^* - k_{Te}^* \big) + \Big(i \frac{\nu_{en}}{\Omega_e} + i \frac{\nu_{ei}}{\Omega_e} - \frac{a_e^2 k_\parallel^2}{\Omega_e \omega} \Big) \Big(1 + \frac{3 a_e^2 k_\perp}{5\Omega_e \omega} \big(\frac{2}{3} k_{ne}^* - k_{Te}^* \big) \Big) \Big] \Big\}$$

$$\zeta_e^y = -i \frac{1}{D_e} \Big\{ \Big[\frac{\nu_{en}}{\Omega_e} (\eta_n^x \xi_i^z + \eta_n^y \eta_i^z + \eta_n^z \zeta_i^z) + \frac{\nu_{ei}}{\Omega_e} \eta_i^z \Big] \cdot$$

$$\cdot \Big(i \frac{\nu_{en}}{\Omega_e} + i \frac{\nu_{ei}}{\Omega_e} - \frac{a_e^2 k_\perp^2}{\Omega_e \omega} \Big) \Big(i \frac{\nu_{en}}{\Omega_e} + i \frac{\nu_{ei}}{\Omega_e} - \frac{a_e^2 k_\parallel^2}{\Omega_e \omega} \Big) - \frac{a_e^4 k_\perp^2 k_\parallel^2}{\Omega_e^2 \omega^2} \Big]$$

$$+ \Big[\frac{\nu_{en}}{\Omega_e} (\zeta_n^x \xi_i^z + \zeta_n^y \eta_i^z + \zeta_n^z \zeta_i^z) + \frac{\nu_{ei}}{\Omega_e} \zeta_i^z - 1 \Big] \Big[i \frac{a_e^2 k_\perp k_\parallel}{\Omega_e \omega} \cdot$$

$$\cdot \Big(1 + \frac{3 a_e^2 k_\perp}{5\Omega_e \omega} \big(\frac{2}{3} k_{ne}^* - k_{Te}^* \big) \Big) + i \frac{3 a_e^2 k_\parallel}{5\Omega_e \omega} \big(\frac{2}{3} k_{ne}^* - k_{Te}^* \big) \cdot$$

$$\cdot \Big(i \frac{\nu_{en}}{\Omega_e} + i \frac{\nu_{ei}}{\Omega_e} - \frac{a_e^2 k_\perp^2}{\Omega_e \omega} \Big) \Big] + \Big[\frac{\nu_{en}}{\Omega_e} (\xi_n^x \xi_i^z + \xi_n^z \eta_i^z + \xi_n^z \zeta_i^z)$$

$$+ \frac{\nu_{ei}}{\Omega_e} \xi_i^z \Big] \Big[i \frac{3 a_e^4 k_\parallel^2 k_\perp}{5\Omega_e^2 \omega^2} \big(\frac{2}{3} k_{ne}^* - k_{Te}^* \big) + \Big(\frac{\nu_{en}}{\Omega_e} + i \frac{\nu_{ei}}{\Omega_e}$$

$$- \frac{a_e^2 k_\parallel^2}{\Omega_e \omega} \Big) \Big(1 + \frac{3 a_e^2 k_\perp}{5\Omega_e \omega} \big(\frac{2}{3} k_{ne}^* - k_{Te}^* \big) \Big) \Big] \Big\}$$

$$\zeta_e^z = i\,\frac{i}{D_e}\left\{\left[\frac{\nu_{en}}{\Omega_e}\left(\eta_n^x\,\xi_i^y + \eta_n^y\,\eta_i^y + \eta_n^z\,\zeta_i^y\right) + \frac{\nu_{ei}}{\Omega_e}\,\eta_i^y - 1\right]\cdot\right.$$

$$\cdot\left[\left(i\,\frac{\nu_{en}}{\Omega_e} + i\,\frac{\nu_{ei}}{\Omega_e} - \frac{a_e^2 k_\perp^2}{\Omega_e\omega}\right)\left(i\,\frac{\nu_{en}}{\Omega_e} + i\,\frac{\nu_{ei}}{\Omega_e} - \frac{a_e^2 k_\parallel^2}{\Omega_e\omega}\right) - \frac{a_e^4 k_\perp^2 k_\parallel^2}{\Omega_e^2\omega^2}\right]$$

$$+\left[\frac{\nu_{en}}{\Omega_e}\left(\zeta_n^x\,\xi_i^y + \zeta_n^y\,\eta_i^y + \zeta_n^z\,\zeta_i^y\right) + \frac{\nu_{ei}}{\Omega_e}\,\zeta_i^y\right]\left[i\,\frac{a_e^2 k_\perp k_\parallel}{\Omega_e\omega}\cdot\right.$$

$$\cdot\left(1 + \frac{3a_e^2 k_\perp}{5\Omega_e\omega}\left(\frac{2}{3}\,k_{ne}^* - k_{Te}^*\right)\right) + i\,\frac{3a_e^2 k_\parallel}{5\Omega_e\omega}\left(\frac{2}{3}\,k_{ne}^* - k_{Te}^*\right)\cdot$$

$$\left.\cdot\left(i\,\frac{\nu_{en}}{\Omega_e} + i\,\frac{\nu_{ei}}{\Omega_e} - \frac{a_e^2 k_\perp^2}{\Omega_e\omega}\right)\right] + \left[\frac{\nu_{en}}{\Omega_e}\left(\xi_n^x\,\xi_i^y + \xi_n^y\,\eta_i^y + \xi_n^z\,\zeta_i^y\right)\right.$$

$$\left.+\frac{\nu_{ei}}{\Omega_e}\,\xi_i^y\right]\left[i\,\frac{3a_e^4 k_\parallel^2 k_\perp}{5\Omega_e^2\,\omega^2}\left(\frac{2}{3}\,k_{ne}^* - k_{Te}^*\right) + \left(i\,\frac{\nu_{en}}{\Omega_e} + i\,\frac{\nu_{ei}}{\Omega_e}\right.\right.$$

$$\left.\left.-\frac{a_e^2 k_\parallel^2}{\Omega_e\omega}\right)\left(1 + \frac{3a_e^2 k_\perp}{5\Omega_e\omega}\left(\frac{2}{3}\,k_{ne}^* - k_{Te}^*\right)\right)\right]\Bigg\}$$

and

$$D_e = -\left(\frac{\nu_{en}}{\Omega_e} + \frac{\nu_{ei}}{\Omega_e}\right)\left(\frac{\nu_{en}}{\Omega_e} + \frac{\nu_{ei}}{\Omega_e} + i\,\frac{a_e^2 k^2}{\Omega_e\omega}\right)\left(i\,\frac{\nu_{en}}{\Omega_e} + i\,\frac{\nu_{ei}}{\Omega_e}\right.$$

$$\left. - \frac{6\,a_e^2\,k_{ne}^*\,k_{Te}^*}{5\Omega_e\omega}\right) + \frac{3a_e^4\,k_\parallel^2 k_\perp}{5\Omega_e^2\omega^2}\left[\frac{1}{3}\,k_{ne}^* + \frac{6a_e^2 k_\perp}{5\Omega_e\omega}\left(k_{ne}^* - k_{Te}^*\right)\right.$$

$$\left.\cdot\left(\frac{2}{3}\,k_{ne}^* - k_{Te}^*\right)\right] - \left[1 - \frac{3a_e^2 k_\perp}{5\Omega_e\omega}\left(k_{ne}^* - k_{Te}^*\right)\right]\left[1 + \frac{3a_e^2 k_\perp}{5\Omega_e\omega}\cdot\right.$$

$$\left.\cdot\left(\frac{2}{3}\,k_{ne}^* - k_{Te}^*\right)\right]\left(i\,\frac{\nu_{en}}{\Omega_e} + i\,\frac{\nu_{ei}}{\Omega_e} - \frac{a_e^2 k_\parallel^2}{\Omega_e\omega}\right) + \frac{9a_e^4 k_\parallel^2}{25\Omega_e^2\omega^2}\cdot$$

(Continued on next page)

$$\cdot (k^*_{ne} - k^*_{Te}) \left(\frac{2}{3} k^*_{ne} - k^*_{Te}\right) \quad \left(i \frac{\nu_{en}}{\Omega_e} + i \frac{\nu_{ei}}{\Omega_e} - \frac{a_e^2 k_\perp^2}{\Omega_e \omega}\right) .$$

CHAPTER IV

TIME-DEPENDENT NEUTRAL WIND STRUCTURE IN THE AURORAL E REGION*

IV-1 Introduction

Recently, Brekke, et al. (1973) presented neutral winds in the auroral E Region, deduced from measurements of the ion drift velocity at different altitudes by the incoherent scatter radar facility at Chatanika, Alaska. Because of experimental limitations, only two data points per profile, corresponding to 110 km and 167 km, lie approximately within the E Region. These values are weighted averages over several tens of kilometers in altitude so that no structure between these altitudes is available. In this study a theoretical model is constructed in an attempt to determine the neutral wind structure in this region.

*This work was done by S. T. Wu and R. H. Comfort. Portions of the results are published in the Proceedings of International Conference on Recent Advances in the Physics and Chemistry of the E-Region (Ed. by S. Matsushita and L. G. Smith), August 1974.

IV-2 Analysis

The model developed is based on electric fields as the primary driving force for the ions, with momentum transferred from the ions to the neutral gas through collisions driving the neutral wind. Both Fedder and Banks (1972) and Heaps (1972) have demonstrated that viscosity in the neutral gas is important, even at E Region altitudes, in redistributing momentum vertically; viscosity is therefore included in the neutral equation of motion. In addition, Heaps (1972) has shown that the coriolis force is important in changing the direction of the neutral wind over the time scale of interest (several hours); this force is also included in the neutral equation of motion. In this initial state of model development pressure gradient terms are neglected, as are the continuity and energy equations. Model values are used for the densities and temperatures governed by these equations. Gravitational forces are assumed to be balanced by vertical pressure gradients in the static diffusion models from which model values are obtained; therefore, as a first approximation, gravity and the vertical pressure gradient are not included explicitly in the vertical equations of motion.

With these assumptions, the governing equations for the present problem are the ion equation of motion

$$\frac{\partial \vec{v}_i}{\partial t} = \frac{e}{\bar{m}_i}\left(\vec{E} + \frac{\vec{v}_i}{c} \times \vec{B}\right) - \bar{\nu}_{in}(\vec{v}_i - \vec{v}_n) \qquad (1)$$

and the neutral equation of motion

$$\frac{\partial \vec{v}_n}{\partial t} = -\frac{1}{\rho_n} \nabla \cdot \overline{\overline{\tau}} - \bar{\nu}_{ni}(\vec{v}_n - \vec{v}_i) + 2\vec{v}_n \times \vec{\Omega}_E \qquad (2)$$

where $\overline{\overline{\tau}}$ is the stress tensor, given by

$$\tau_{ij} = -\eta \left[\frac{\partial v_i}{\partial x_j} + \frac{\partial v_j}{\partial x_i} \right] + \frac{2}{3} \eta \, \delta_{ij} \, \nabla \cdot \vec{v}. \qquad (3)$$

In equations (1) - (3) $\vec{v}_i$ and $\vec{v}_n$ are the ion and neutral wind velocities $\bar{\nu}_{in}$ and $\bar{\nu}_{ni}$ are average ion-neutral and neutral-ion collision frequencies, $\vec{E}$ and $\vec{B}$ are the electric and geomagnetic field strengths, $\bar{m}_i$ and ρ_n are the mean ion mass and neutral mass density, η is the coefficient of absolute viscosity, e and c are the electronic charge (magnitude) and speed of light and $\vec{\Omega}_E$ is the earth's angular velocity vector. Horizontal gradients in these quantities are assumed to be negligibly small. Average collision frequencies $\bar{\nu}_{in}$ and $\bar{\nu}_{ni}$ are evaluated in the following way:

$$\bar{\nu}_{in} \equiv \frac{1}{N_e \bar{m}_i} \sum_{r,s} n_r \, \mu_{rs} \, \nu_{rs}$$

$$\bar{\nu}_{ni} = \frac{\rho_i}{\rho_n} \bar{\nu}_{in}$$

where r and s range over all ion and neutral species respectively, μ_{rs} is the reduced mass, and ν_{rs} is the ion-neutral collision frequency for momentum transfer as given by Banks (1966).

For convenience in performing the calculations, the ion equation is treated in the "plasma" coordinate system (Figure 1a) and the neutral equation in a local geographic coordinate system (Figure 1b). The transformations between these coordinate systems for an arbitrary vector $\vec{q}$ are:

(i) From plasma coordinates (1, 2, 3) to local geographic coordinates (x, y, z)

$$q_x = q_2 \sin\delta - \cos\delta\,(q_1 \sin I + q_3 \cos I) \qquad (4a)$$

$$q_y = q_2 \cos\delta + \sin\delta\,(q_1 \sin I + q_3 \cos I) \qquad (4b)$$

$$q_z = q_1 \cos I - q_3 \sin I \qquad (4c)$$

(ii) From local geographic coordinates (x, y, z) to plasma coordinates (1, 2, 3)

$$q_1 = q_z \cos I - \sin I\,(q_x \cos\delta - q_y \sin\delta) \qquad (5a)$$

$$q_2 = q_x \sin\delta + q_y \cos\delta \qquad (5b)$$

$$q_3 = -q_z \sin I - \cos I\,(q_x \cos\delta - q_y \sin\delta) \qquad (5c)$$

The angles I (magnetic dip angle) and δ (magnetic declination angle) are defined by Figure 1c. All results are presented in the local geographic coordinate system.

Because of the high conductivity along magnetic field lines, the electric field $\vec{E}$ is assumed to have no component parallel to the magnetic field and $\vec{E}$ is assumed to be mapped down the field lines without loss or rotation to all altitudes of interest. Brekke, et al., (1973) provides data for the E_x and E_y components of electric field. The assumption of no parallel electric field ($E_3 = 0$) allows equation (5c) to be solved for E_z, giving

$$E_z = -\cot I\,(E_x \cos\delta - E_y \sin\delta)\,. \qquad (6)$$

Since $\vec{E}$ is used only in the plasma coordinate system (1, 2, 3), equation (6) is used together with equation (5) to express E_1 and E_2 in terms of the E_x and E_y data.

In early numerical tests, using an explicit finite difference technique, it was determined that the ion equations of motion come

into a steady state with constant driving forces within a few collision times ($1/\bar{\nu}_{in}$). For the models used, these collision times vary from ~10^{-4} sec at 90 km to ~1 sec at 250 km. Hence, at all altitudes of interest the ions achieve a steady state with driving forces within a few seconds, providing the driving forces vary only slightly during this time. In this problem, the driving force is an electric field which varies significantly only over a period of several minutes (values presented by Brekke, et al. (1973) represent at least 10 minute averages). The time-dependent ion equations can therefore be replaced by the time-independent equations $\left(\frac{\partial \vec{v}_i}{\partial t} = 0\right)$ with little loss of accuracy. Ion component equations in plasma coordinates then have the customary form

$$v_{i1} = \left[\frac{1}{1 + (\bar{\omega}_i/\bar{\nu}_{in})^2}\right]\left[v_{n1} + \frac{\bar{\omega}_i}{\bar{\nu}_{in}}\left(\frac{E_1}{B} c + v_{n2}\right) + \left(\frac{\bar{\omega}_i}{\bar{\nu}_{in}}\right)^2 \frac{E_2}{B} c\right] \quad (7a)$$

$$v_{i2} = \left[\frac{1}{1 + (\bar{\omega}_i/\bar{\nu}_{in})^2}\right]\left[v_{n2} + \frac{\bar{\omega}_i}{\bar{\nu}_{in}}\left(\frac{E_2}{B} c - v_{n1}\right) - \left(\frac{\bar{\omega}_i}{\bar{\nu}_{in}}\right)^2 \frac{E_1}{B} c\right] \quad (7b)$$

$$v_{i3} = v_{n3} \quad (7c)$$

where $\bar{\omega}_i = (eB)/(\bar{m}_i c)$ is the mean ion gyrofrequency. The time dependence of $\vec{v}_i$ is now implicit in the time dependence of $\vec{E}$ and $\vec{v}_n$.

The coupled set of time-independent ion momentum equations (7a)-(7c) and neutral momentum equations (2) is solved numerically, using an explicit finite difference technique, by prescribing a value of the electric field at each time step. As initial conditions, all neutral velocity components are taken to be zero. Boundary conditions at 90 km

are the vanishing of all neutral velocity components, and at 250 km, $\frac{\partial \vec{v}_n}{\partial z} = 0$. These boundary conditions, while not strictly correct, have little effect in the region of interest, 100 km to 200 km. Two different sets of electric field values are considered, a constant electric field and electric field values inferred by Brekke, et al., from data taken with the incoherent scatter radar at Chatanika, Alaska. Model neutral parameters used are obtained from a Jacchia-71 model atmosphere at a constant exospheric temperature of 1000 degrees. Ion densities, both day and night values, are taken from Brekke, et al. (1973). Crude ion composition models for day and night have been formed based on the rocket data of Kopp, et al. (1973). The only time variation associated with these models in the calculations is the use of the night model during hours of darkness for the calculation using Chatanika data, while using the daytime model for all other times. With these models, $\bar{\nu}_{in} = \bar{\omega}_i$ at 122 km.

IV-3 Results

In order to understand more clearly how the ion-neutral system responds to electric fields, a simple case is considered initially. A constant electric field of 20 mV/m is applied for five hours in the + x (south) direction, followed by three hours of zero field. All geometric parameters correspond to the location of Chatanika, Alaska (next example), and daytime model values are used. Figure 2 shows the ion and neutral velocity components as functions of time at altitudes of 115 km, 125 km, and 150 km. The difference in magnitude of the ion components at these altitudes clearly displays the effects of increased collisional coupling with the neutral gas at lower

altitudes. In addition, the inertia of the neutral gas is evident at T = 5 hours, when the electric field driving force is terminated; the "coasting" neutral wind then becomes the driving force for the ions.

To see the altitude structure of the velocity fields, altitude profiles of all velocity components are shown for T = 5 hours in Figure 3a. The same calculation has been performed with the coriolis term set to zero in order to determine the effect of that term on the calculation; resulting profiles are shown in Figure 3b. Comparison with Figure 3a shows clearly that the coriolis force is primarily responsible for the magnitude of the vertical components. This force is also seen to cause a redistribution of momentum among the horizontal neutral velocity components, with consequent effects on the ion velocity. A similar calculation setting the viscous terms to zero gives results (not shown) very similar to Figure 3a. The primary effects of viscous terms are found to be a small damping of the vertical components and a minor smoothing of the altitude profiles.

For more realistic time variations, electric fields determined by Brekke, et al. (1973), from incoherent scatter radar observations at Chatanika, Alaska ($L \simeq 5.7$, $\Lambda = 65°$, $I = 76.5°$, $\delta = 29°$) for July 10-11, 1972, are used. These electric field values are shown in Figure 4a (note that here +x is south, while Brekke, et al. (1973), used positive values for north). Determination of electric field values was made from high altitude ion drift measurements, while lower altitude ion drift measurements were used to deduce neutral winds. The technique for the latter determination, described in detail by Brekke, et al. (1973), results in a weighted height-integrated value for neutral winds

with the primary weighting in the 110 km to 120 km region, but varying with the ion density profile. These neutral wind values from Brekke, et al. (1973) are shown in Figure 4b.

Time variation of ion and neutral wind components, calculated as described above for the electric field of Figure 4a, is shown in Figure 5 for altitudes of 115 km, 125 km, and 150 km. Ion velocity temporal structure parallels that of the electric field while the neutral components vary smoothly, almost sinusoidally in time. Altitude effects are particularly noticeable in the y components. Representative examples of the altitude structure are shown in Figure 6. All ion and neutral velocity components are shown as functions of altitude for 0800 hours UT in Figure 6a and for 1030 hours UT in Figure 6b. These profiles, as those in Figure 3, are characterized by large gradients in the 110 km to 130 km region, and in some cases, a reversal of direction there. Above 140 km the velocity components change rather slowly with altitude, reflecting the reduced collisional coupling in this region.

A comparison of the neutral velocity components in Figure 4b with those in Figure 5, while not strictly appropriate quantitatively, is nevertheless instructive. One notable difference is the relative lack of temporal structure in the calculated components. This qualitative discrepancy should have a physical explanation. If the calculated values for 115 km are used in the comparison, the peak magnitudes agree and the general directions of the x components agree; however, agreement between the y components is rather poor. If a

higher altitude is picked for the calculated y component, agreement in general direction is improved - at the expense, however, of agreement in general magnitude.

With this comparison as a background, several shortcomings of these calculations can be examined qualitatively. In the present treatment only two representative ion density altitude profiles are used (for day and night conditions), whereas the data analysis of Brekke, et al. (1973) employed profiles measured simultaneously with the ion drift measurements. The high variability of these profiles is illustrated in data presented by Banks, et al. (1974). Although inclusion of this variability (through $\bar{\nu}_{ni}$) in the neutral equation of motion could modify the calculated neutral winds somewhat, the result would probably be similar to that due to electric field variations, which enter the neutral equations through ion velocity variations in the collision term. Figure 5 demonstrates that such short period variations are effectively filtered out of the neutral components, due to the large inertia of the neutral gas relative to the ion gas. Furthermore, the tendency of electric fields and E region ionization densities to be anticorrelated (Banks, et al., 1974) would have a compensating effect in the collision terms of the neutral equations, reducing the effective magnitude of variations in these terms.

Another omission of the present calculation is horizontal pressure gradients. It is reasonable to expect large short term variations in such pressure gradients associated with corresponding large variations in Joule heating in the auroral oval. However, no data is available to provide information on these pressure gradients for the time and

location treated. There is also little theoretical work to suggest how far from the source region significant pressure gradients might extend. In addition to the large variable pressure gradients associated with Joule heating, smaller pressure gradients due to diurnal thermal tides would bias the results, particularly when electric fields are small. For the present calculation, this effect is not expected to modify the results to a large extent.

Based on the comparison of Figure 4b and 5 above, it appears that the effective altitude of the measurement may be varying. Since it is the ion drift which is measured, the altitude structure of the ion velocity components must enter into the weighting which determines the altitude region contributing most significantly to the measured results. Figures 3 and 6 show that below 110 km velocities are small, increasing rapidly with altitude to about 130 km and less rapidly above that. In addition reversals of velocity component directions in the 110 km to 130 km region would effectively cause cancellations in the lower altitude contributions to the integrated results, further raising the effective contributing altitude region. If these shifts occur within the region of large vertical gradients, it appears that significant differences in the weighted integrated results could occur. Examination of Figure 5 indicates that ion velocity altitude structure can change very rapidly in response to changing electric fields. This variability coupled with the variability of ion density altitude profiles, both of which affect the altitude weighting of the integrated velocity measurement, could be factors in explaining the temporal structure of the neutral velocities deduced from measured ion velocities (Figure 4b). These qualitative arguments require quantitative support;

calculations of this nature are in progress.

Finally, the vertical velocity components of 100 m/s or more, evident in all of the calculated results (Figures 3, 5 and 6), require comment. Comparison of Figures 3a and 3b has established that the coriolis term is a primary source of these velocities. However, measured ion vertical velocities are typically less than 50 m/s (Banks, et al. 1974; Rieger, 1974). The assumption of total cancellation between the vertical pressure gradient and gravitational acceleration is clearly not a good one for the dynamic case. Order of magnitude estimates indicate that in the ion equation, these terms are smaller than those included by factors of 10^2 to 10^5. However, in the neutral equation, the gravity term is 10^3 times larger than the terms included, so that even a small perturbation of the hydrostatic pressure can have a very significant affect on vertical velocities. Pressure perturbations due to vertical driving forces must therefore be included in a realistic treatment of vertical winds; and this requires inclusion of the continuity and energy equations in the set of equations to be solved. The qualitatively significant result remains, however: large horizontal winds mean significant vertical driving forces are present.

IV-4 Conclusions

Over time scales of several hours, the coriolis force plays a significant role in redirecting the neutral wind, including driving a vertical component; for these time scales this force should be included in the neutral equations of motion. Ion velocities respond rapidly to changing electric fields at all altitudes so that vertical structure of these velocities can change quickly. Resulting changes

in the neutral velocity altitude structure, however, require one to two hours, due to the greater neutral gas density. In these calculations, ion and neutral velocities are small (below 110 km), increase in magnitude rapidly with altitude to about 130 km, and change more slowly with altitude above. This variability of ion velocity altitude structure may complicate the interpretation of weighted height-integrated ion velocity measurements. Realistic treatment of vertical velocities requires explicit consideration of pressure perturbations resulting from vertical motion; in general this will require inclusion of the continuity and energy equations in the system of equations.

Finally, we may conclude from the present calculation that the effects of coriolis force are clearly indicated. A strong shear layer appeared in the neutral wind profiles. However, the Richardson number may still very well be in the laminar flow region.

REFERENCES

Banks, P. M. (1966), "Collision Frequencies and Energy Transfer-Ions," Planet. Space Sci., Vol. 14, 1105.

Banks, P. M., Rino, C. L., and Wickwar, V. B. (1974), "Incoherent Scatter Radar Observations of Westward Electric Fields and Plasma Densities in the Auroral Ionosphere, 1," J. Geophys. Res. 79, 187.

Brekke, A., Doupnik, J. R., and Banks, P. M. (1973), "A Preliminary Study of the Neutral Wind in the Auroral E Region," J. Geophys. Res. 78, 8235.

Fedder, J. A., and Banks, P. M. (1972), "Convection Electric Fields and Polar Thermospheric Winds," J. Geophys. Res. 77, 2328.

Heaps, M. G. (1972), "Circulation in the High Altitude Thermosphere Due to Electric Fields and Joule Heating," Doctoral Dissertation, Utah State University.

Kopp, E., Eberhardt, P., and Geiss, J. (1973), "Ion Composition in the E- and Lower F-Region Above Kiruna During Sunset and Sunrise," Planet. Space Sci. 21, 227.

Rieger, E. (1974), "Neutral Air Motions Deduced from Barium Releases Experiments - I, Vertical Winds," J. Atmosph. Terr. Phys. 36, 1377.

FIGURE CAPTIONS

Figure IV-1 Definitions of coordinate systems used in the calculation and the angles relating them.

Figure IV-2 Ion and neutral velocity components as functions of time for altitudes 115 km, 125 km and 150 km for the constant electric field: E_x = 20 mV/m, T $\leq$ 5 hours; E_x = 0, T > 5 hours; E_y = 0, all T.

Figure IV-3 Altitude profiles of ion and neutral velocity components at T = 5 hours for the electric field defined for Fig. 2: (a) all terms in equation (2); (b) omitting coriolis term from equation (2).

Figure IV-4 Data determined from observations by the incoherent scatter radar at Chatanika, Alaska, on 10-11 July 1972 (from Brekke, et al. 1973). (From 9730 to 0900 hours UT, no data was reported; electric fields for that period are sketched in graphically for continuity in the calculation.) (a) electric fields; (b) neutral wind velocities.

Figure IV-5 Calculation ion and neutral velocity components as functions of time for altitudes 115 km, 125 km, and 150 km due to electric fields of Fig. 4a.

Figure Iv-6 Representative calculated altitude profiles of ion and neutral velocity components due to electric fields of Fig. 4a. (a) for UT = 0800 hours; (b) for UT = 1030 hours.

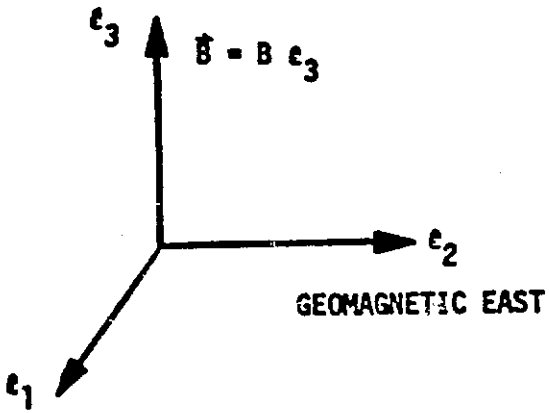

PLASMA COORDINATES

(1a)

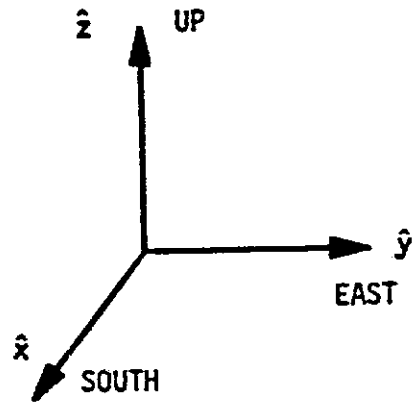

LOCAL GEOGRAPHIC COORDINATES

(1b)

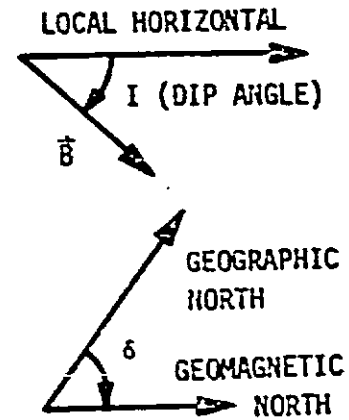

(1c)

Figure IV-1

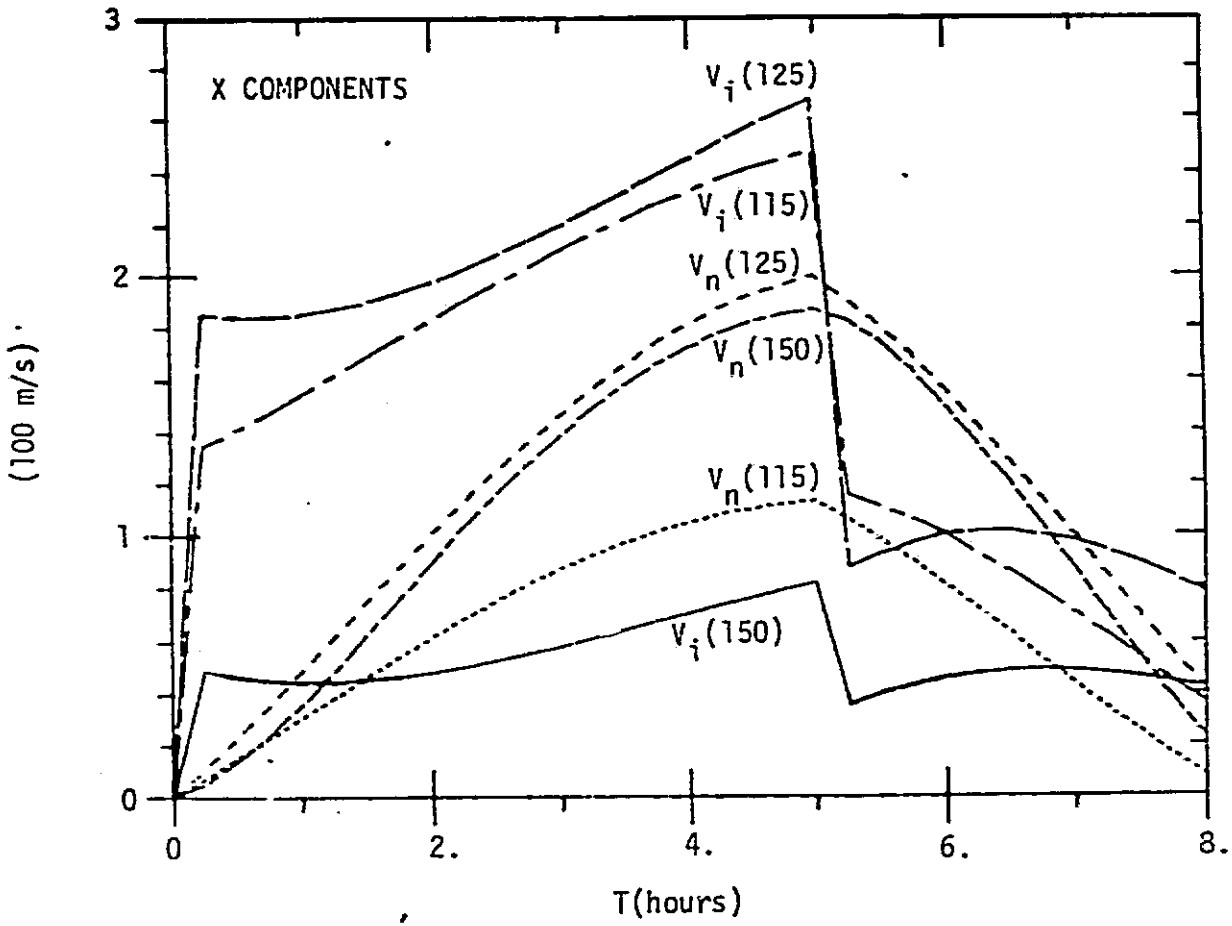

Figure IV-2(a) (x-component)

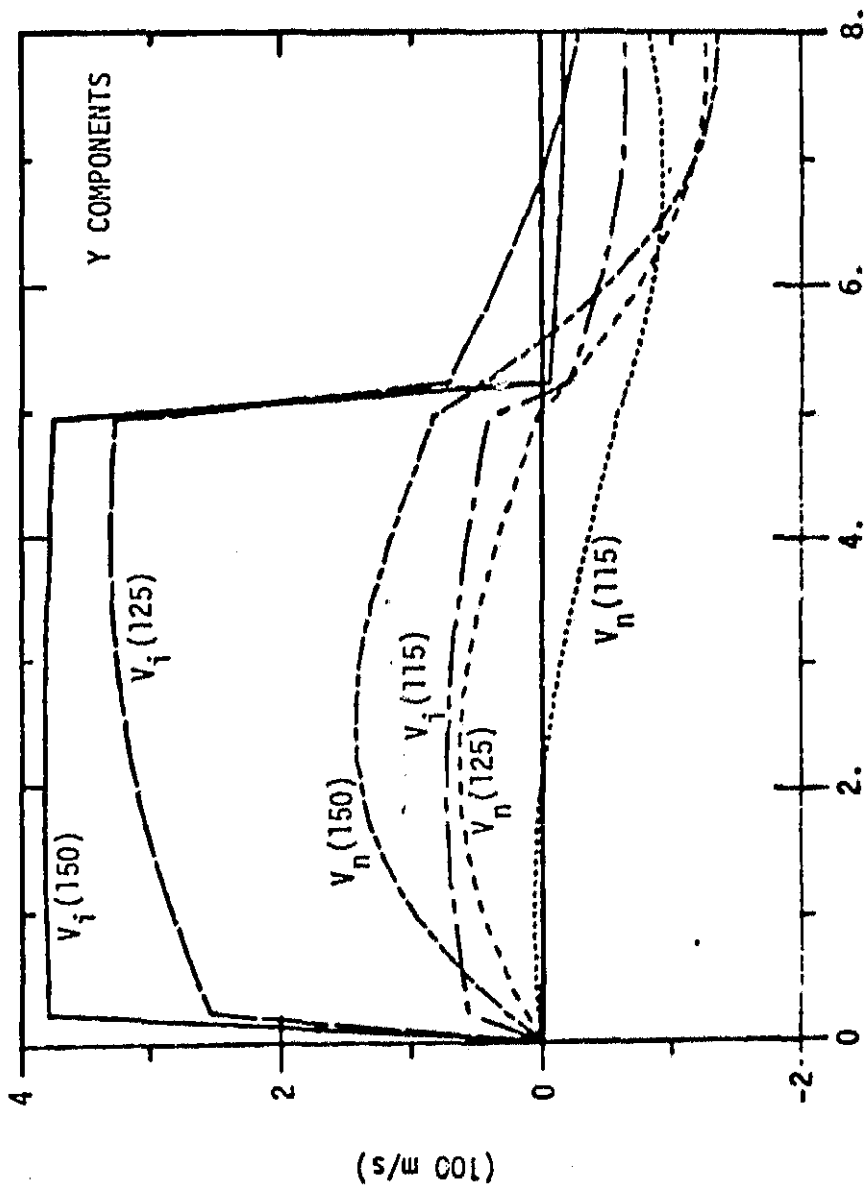

Figure IV-2(b) (y-component)

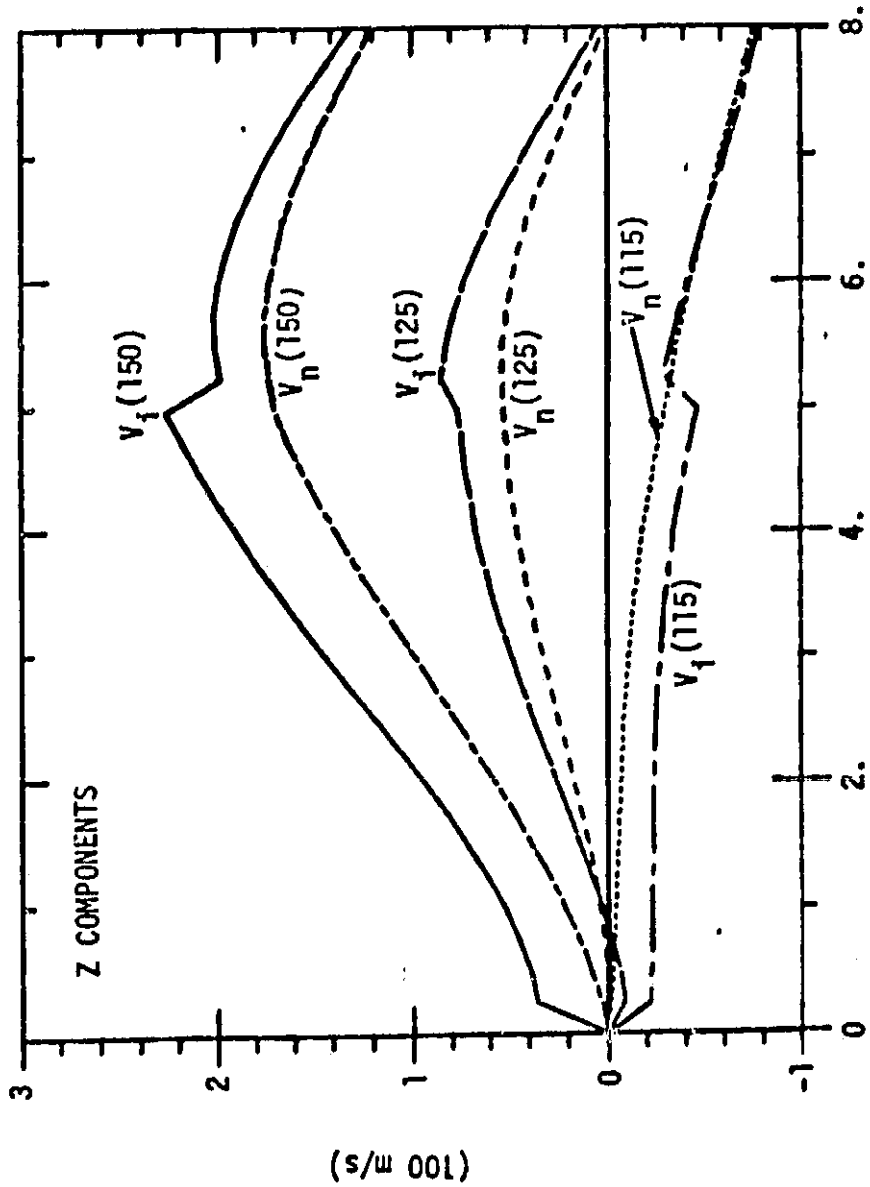

Figure IV-2(c) (z-component)

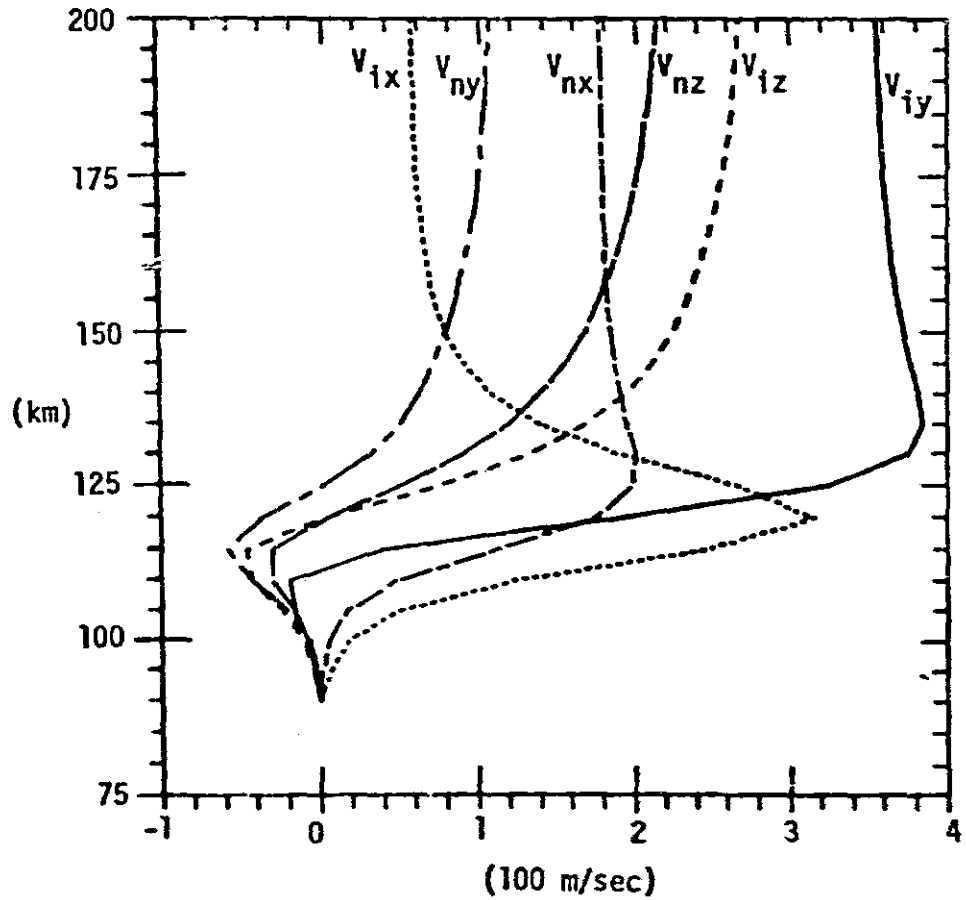
200
175
150
125
100
75
(km)
V_{ix}
V_{ny}
V_{nx}
V_{nz}
V_{iz}
V_{iy}
-1
0
1
2
3
4
(100 m/sec)

Figure IV-3(a)

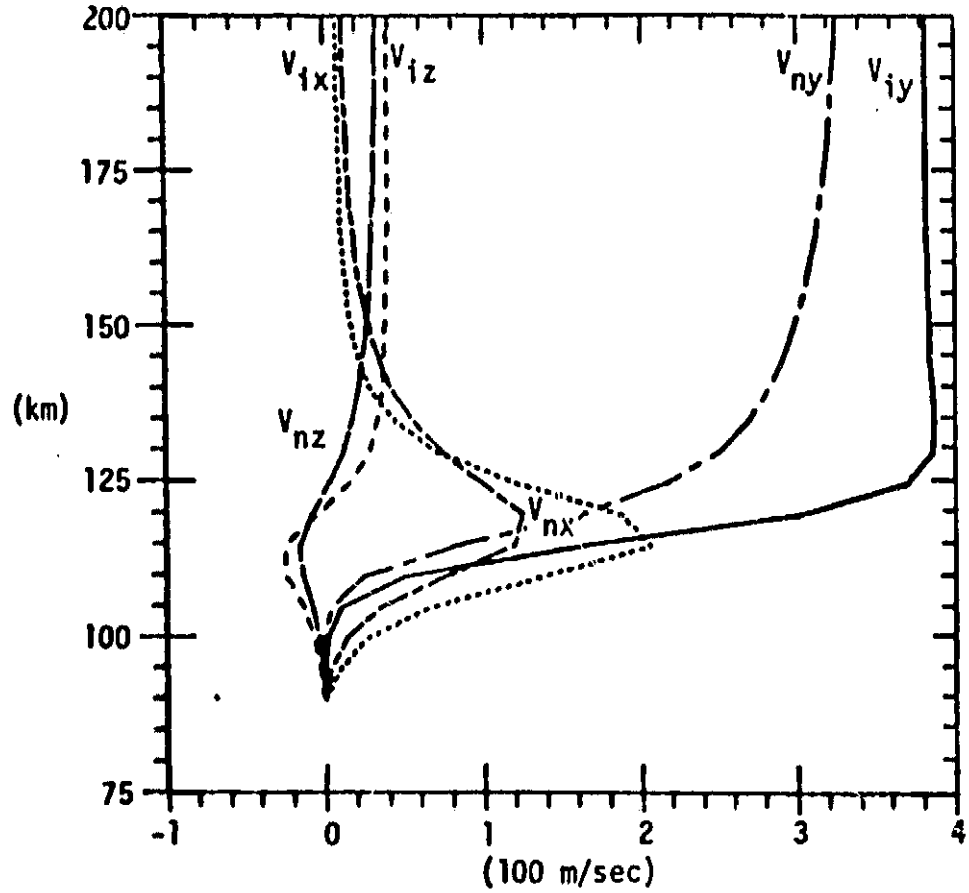
200
175
150
125
100
75
(km)
V_{ix}
V_{iz}
V_{ny}
V_{iy}
V_{nz}
V_{nx}
-1
0
1
2
3
4
(100 m/sec)

Figure IV-3(b)

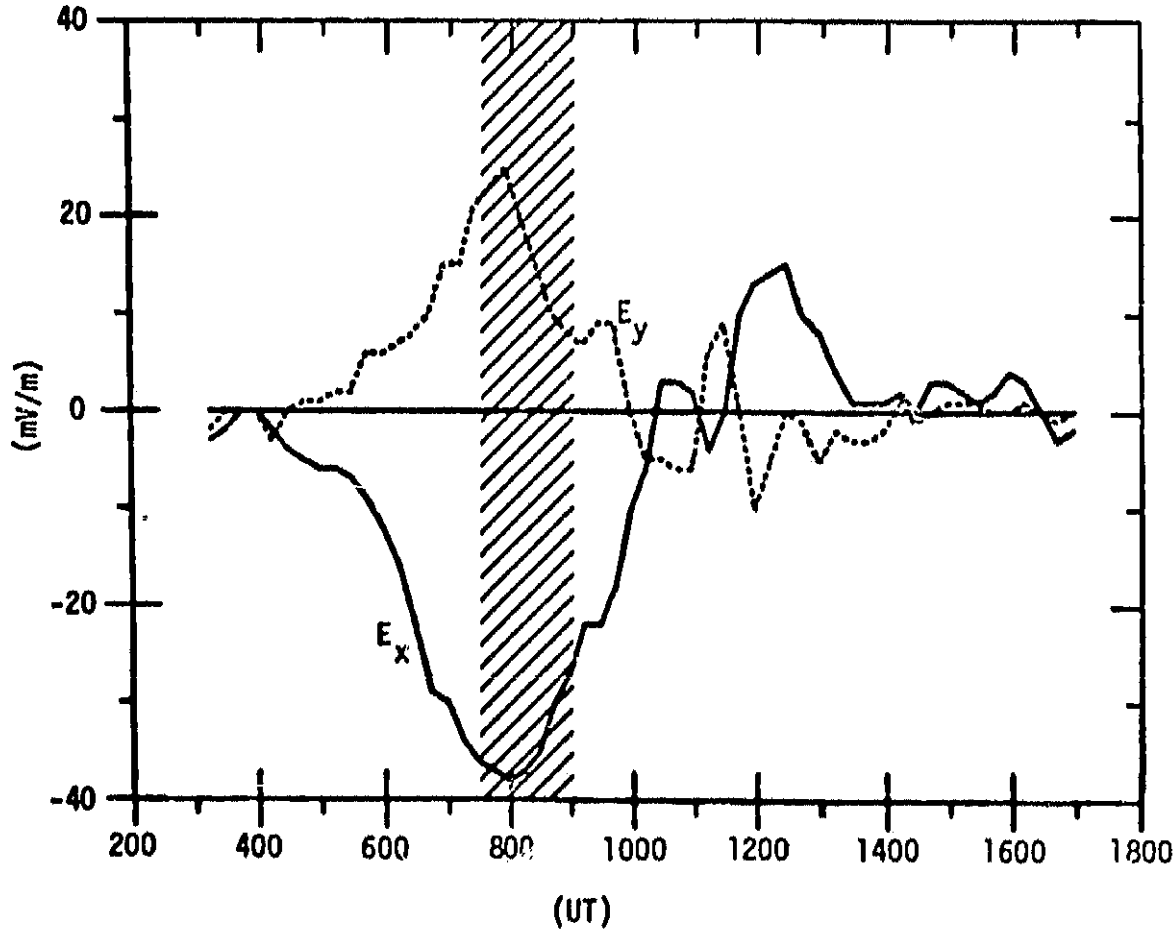
40
20
0
-20
-40
(mV/m)
E_y
E_x
200
400
600
800
1000
1200
1400
1600
1800
(UT)

Figure IV-4(a)

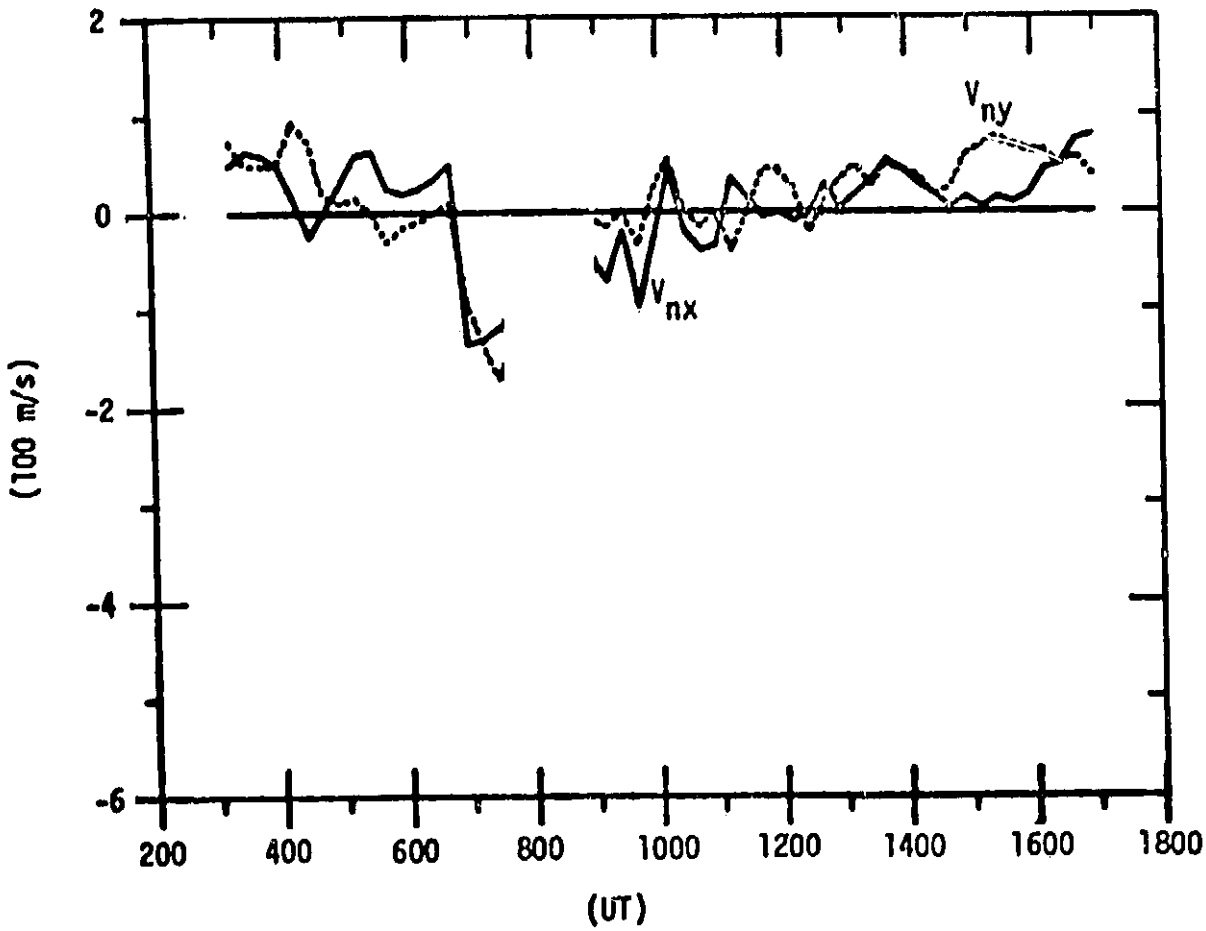
2
0
-2
-4
-6
(100 m/s)
200
400
600
800
1000
1200
1400
1600
1800
(UT)
V_{ny}
V_{nx}

Figure IV-4(b)

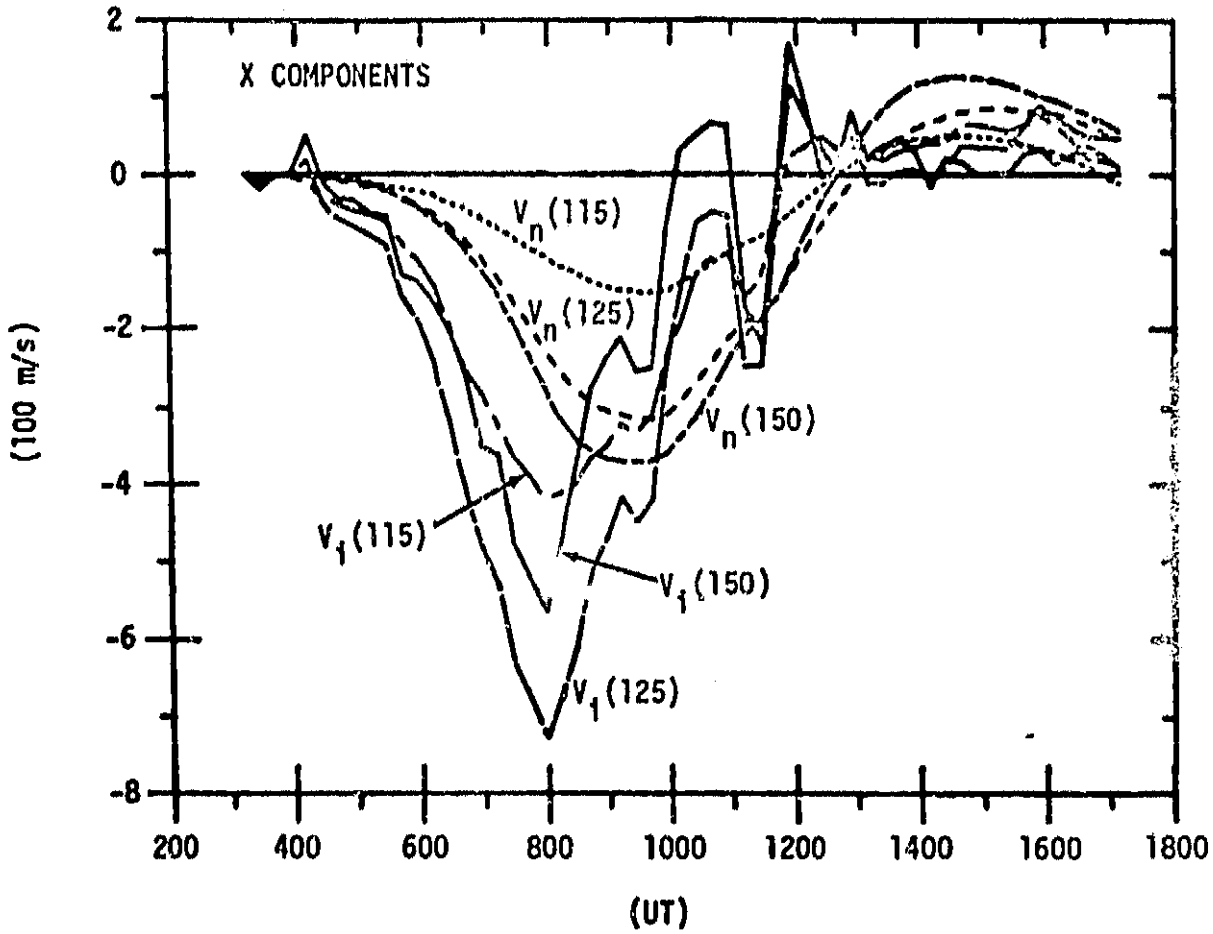

Figure IV-5(a) (X-component)

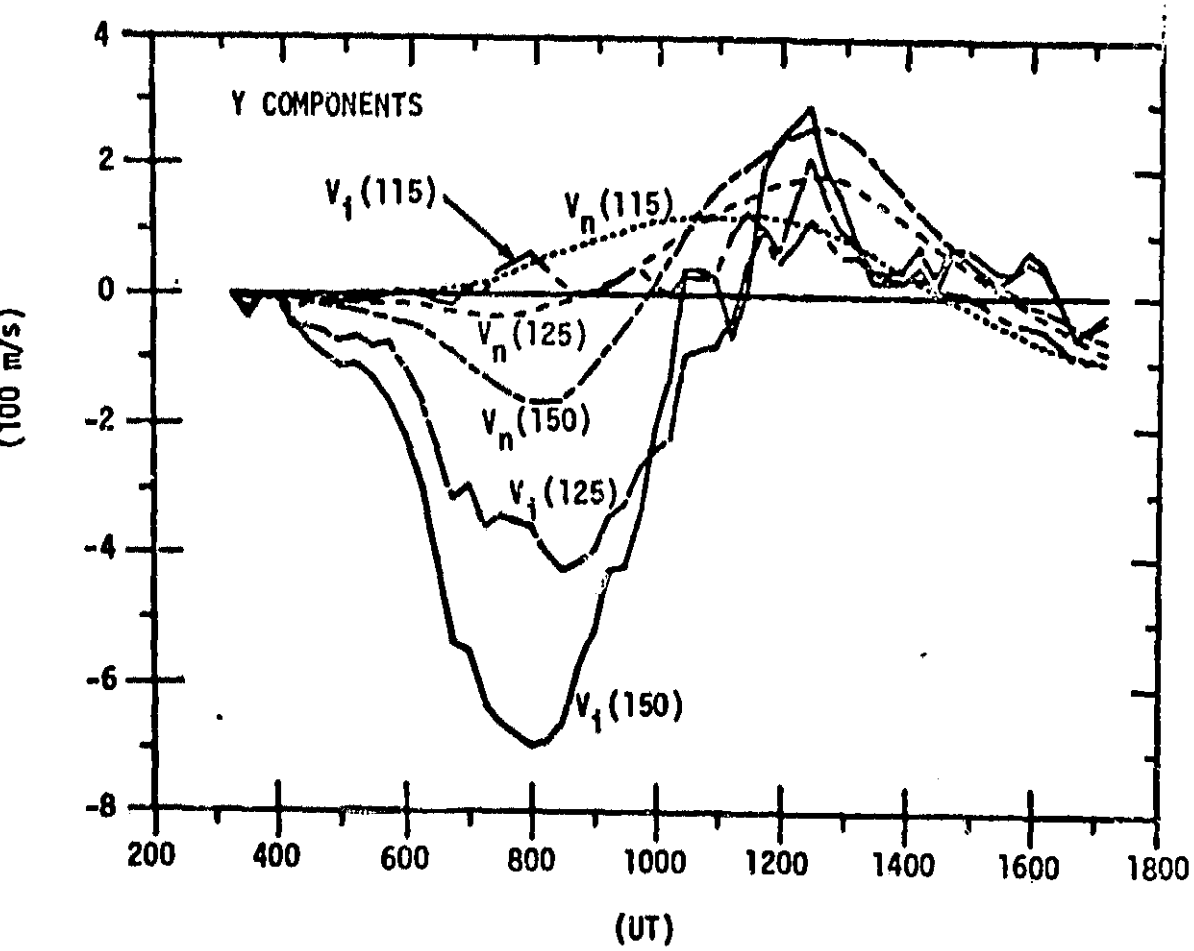

Figure IV-5(b) (y-component)

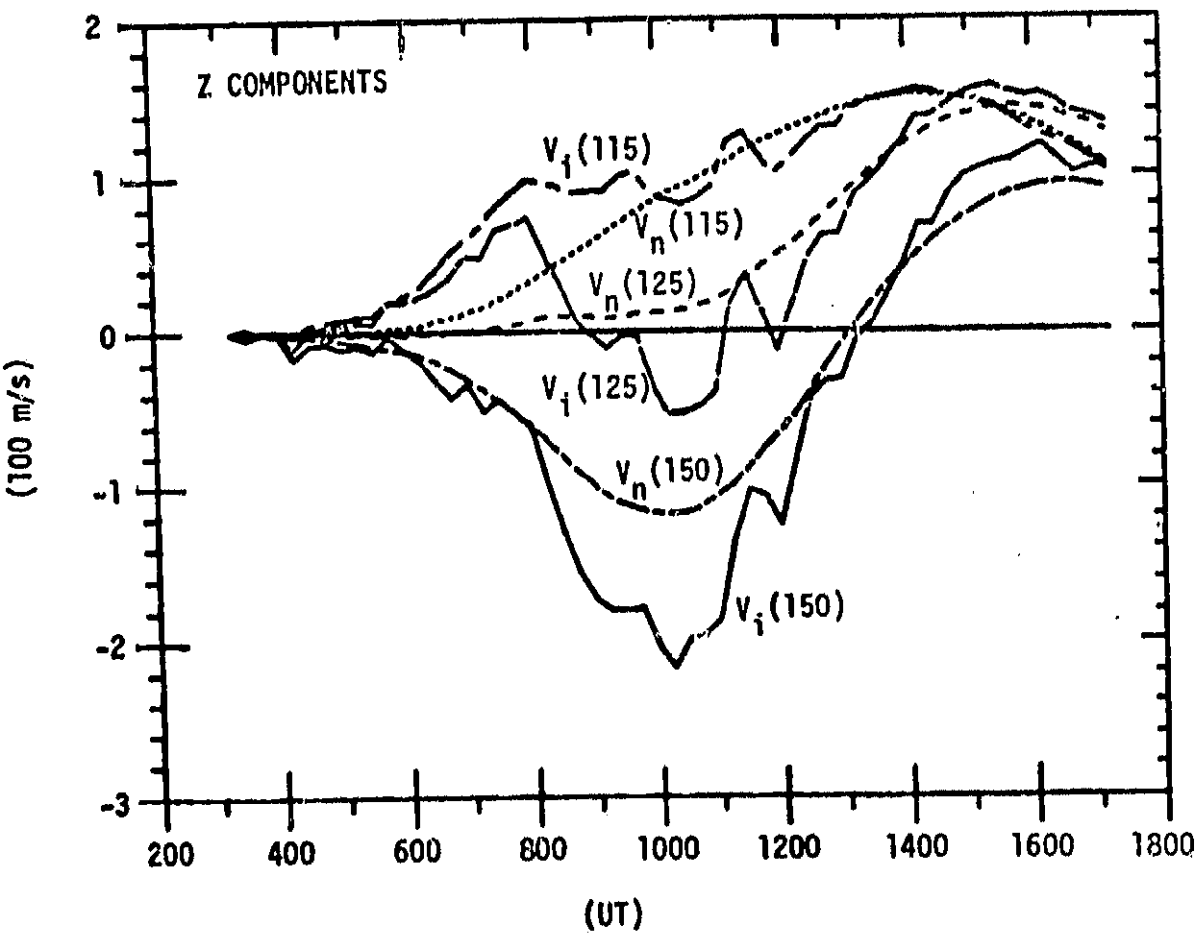

Figure IV-5(c) (z-component)

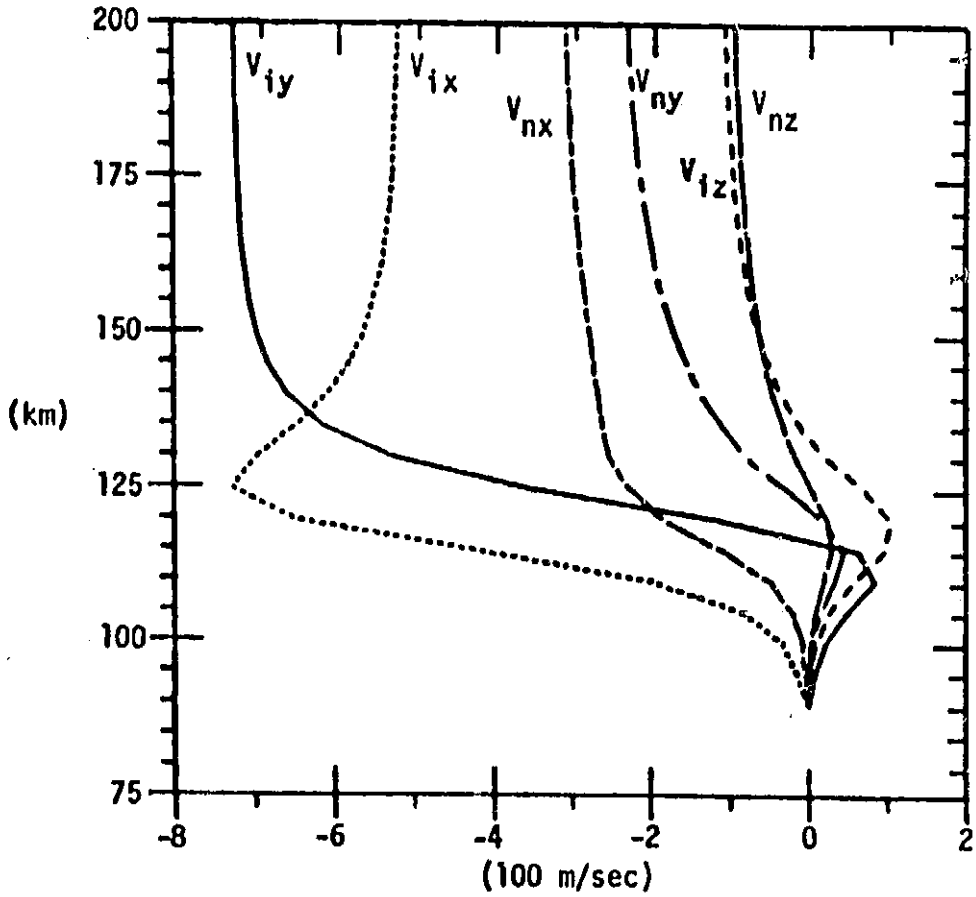
200
175
150
125
100
75
(km)
V_{iy}
V_{ix}
V_{nx}
V_{ny}
V_{nz}
V_{iz}
-8
-6
-4
-2
0
2
(100 m/sec)

Figure IV-6(a)

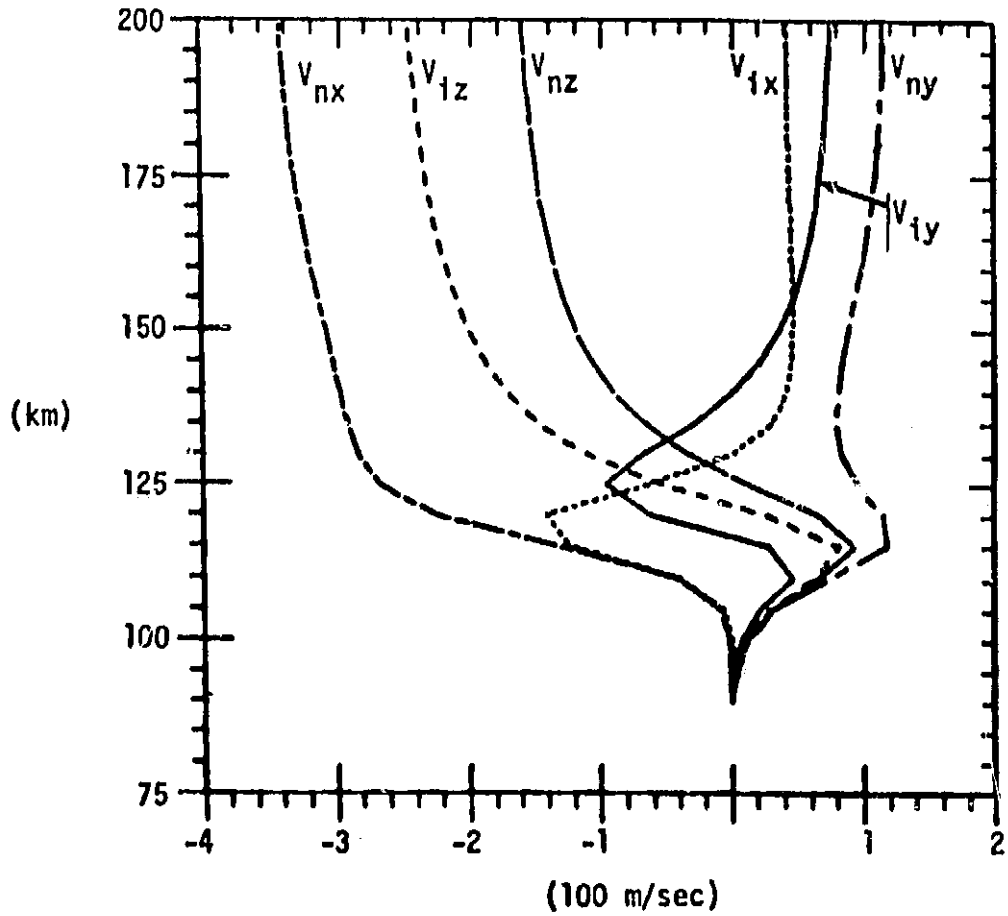
200
175
150
125
100
75
(km)
V_{nx}
V_{iz}
V_{nz}
V_{ix}
V_{ny}
V_{iy}
-4
-3
-2
-1
1
2
(100 m/sec)

Figure IV-6(b)

CHAPTER V

CONCLUDING REMARKS

In this study we have presented a multifluids plasma model for the ionosphere in the region of 90-2,000 Km. The wide range of density and temperature distributions will lead to a wide-range distribution of the collision frequencies among the species (i.e., electrons, ions and neutrals) at different altitudes. Thus, the physics of the dynamical behavior in this region can be classified based on these parameters (i.e., density, temperature and collision frequency). Subsequently, the proper equations to govern the physical phenomena can be obtained.

In the present study, we have presented only three examples demonstrating the theory developed which will enable us to study the wide range dynamical phenomena in the upper atmosphere (90 - 2,000 Km), including the lower part of the magnetosphere. Again, there are many interesting problems observed in the ionosphere and magnetosphere regions. We shall mention a few which form a basis for future study. These are:

i) Utilize the present model to study the joule heating effects in relation to the upper atmospheric dynamics.

ii) The detailed examination of the instability mechanism as an altitude dependence should be very interesting; it could be possible to shed some light concerning the triggering mechanism of the ionospheric irregularities.

iii) All the examples presented are limited to the local coordinate system. It is important to extend the present model to the global scale.